Geological Quarterly, 2021, 65: 28
DOI: http://dx.doi.org/10.7306/gq.1597

U-Th ages and facies properties of Edremit travertines and tufas, Van, Eastern Anatolia: implications for the neotectonics of the region

Çetin YEŞİLOVA[1, *], Pelin GÜNGÖR YEŞİLOVA[1], Mustafa AÇLAN[1], Tsai-Luen YU[2, 3] and Chuan-Chou SHEN[2, 3, 4]

[1] Yüzüncü Yıl University, Department of Geological Engineering, 65080, Van, Turkey

[2] High-precision Mass Spectrometry and Environment Change Laboratory (HISPEC), Department of Geosciences, National Taiwan University, Taipei 10617, Taiwan

[3] Research Center for Future Earth, National Taiwan University, Taipei 10617, Taiwan

[4] Global Change Research Center, National Taiwan University, Taipei 10617, Taiwan

Yeşilova, Ç., Güngör Yeşilova, P., Açlan, M., Yu, T.-L., Shen, Ch.-Ch., 2021. U-Th ages and facies properties of Edremit travertines and tufas, Van, Eastern Anatolia: implications for the neotectonics of the region. Geological Quarterly, 65: 28, doi: 10.7306/gq.1597

Travertine formation is one of the most important archives of active tectonics in a region and provides information about climate, water temperature and quantity, and biological activity. The Edremit travertines and tufas extend over nearly160 km^2 within the boundaries of the Edremit area to the east of Lake Van (eastern Turkey), and yield important evidence towards understanding the neotectonics of the region. The Edremit travertines and tufas were studied throughout their full stratigraphic extent, the factors controlling the formation of these deposits were examined, and the succession was sampled for U/Th analysis. Travertine formation was found to occur from 542–29.7 ka, with two different tufa formation periods: from 29.7–5.8 ka and 5.8–2.08 ka. Pauses in travertine formation (palaeosols) were identified from 510–470 ka, 289–269 ka and 91–34 ka. Our study showed that climate parameters affected the formation of tufa, while the Edremit travertines developed under the control of tectonism. The Van Fault is directly associated with travertine development and its age was identified as 542 ka or older. Since the Gürpınar Fault, one of the most important faults in the region, is effective in shaping the southern slope of the travertines and limiting the movement of the Van Fault, its age should be younger than 542.4 ka. The Elmalık Fault played an active role in the formation of the Edremit tufas and is proposed to be 29.7 ka in age, from stratigraphic relationships in the region.

Key words: palaeosol, travertine facies, Van Fault, tufa, growth rate, Lake Van.

INTRODUCTION

Travertine is the name given to calcium carbonate rock accumulating in areas where warm water rich in calcium and bicarbonate reaches the surface through fractures, joints or active fault lines (Pedley, 1990; Ford and Pedley, 1996; Guo and Riding, 1998; Pentecost, 2005; Gandin and Cappezuoli, 2008). However, it is known that waters with low calcium carbonate content also precipitate travertine (Luo et al., 2021). Depending on how they are classified morphologically and as regards and lithofacies, travertines are frequently used for tectonic and palaenvironmental interpretations both regionally and at small scale. As a result, there are many studies concerning travertines (Altunel and Hancock, 1993b; Guo and Riding, 1998; Fouke et al., 2000; Pentecost, 2005; Veysey et al., 2008; Guido et al., 2010; Guido and Campbell, 2011). Hancock et al. (1999) stated that there is a close relationship between travertine formation and tectonism, and they called such related travertine deposits “travitonic”.

The term tufa was used interchangeably with travertine by many researchers in generally naming freshwater carbonates and cave sediments (Irion and Müller, 1968; Pentecost, 1981; Julia, 1983; Pentecost and Viles, 1994; Viles and Goudie, 1990). However, over time, travertine began to be used for warm and hot water carbonates (Pedley, 1990; Pentecost and Viles, 1994; Pentecost, 2005; Jones and Renaut, 2010), and tufa as cold water carbonates (Pedley, 1990; Koban and Schweigert, 1993; Pentecost, 2005; Gandin and Cappezuoli, 2008). Cappezuoli et al. (2014) defined tufas as phytoherm carbonates with very high biological content, with weak layers, forming in water generally <20°C, and with porosity >40%. Thus, travertine and tufa are now clearly represent separate deposit types. In some geothermal systems, sediments identical to tufa are observed at the margins of travertine deposits, reflecting cooling of the water as the thermal waters become more distant from the source. Cappezuoli et al. (2014) proposed the term “travitufa” for these deposits.

* Corresponding author, e-mail: cetinyesilova@gmail.com

Received: August 17, 2021; accepted: April 22, 2021; first published online: 21 June, 2021

Palaeosol is the name given to ancient soils formed as a result of physical, chemical and biological processes at the rock surface (Kraus, 1999; Retallack, 2014; Tabor and Meyers, 2015). Palaeosols, which are formed as an interaction of lithosphere, hydrosphere, biosphere and atmosphere, are extremely important as they record physical, biological and chemical conditions of past times (Tabor and Meyers, 2015). Palaeosols are frequently used in palaeoclimate assessments due to the pollen data they contain and in correlation of Quaternary deposits at local and regional scale due to their distinctive features (e.g., Richmond, 1962; Morrison, 1967; Pecsi, 1995; Pazonyi et al., 2013; Toker Tagliasacchi, 2018). Some travertine and tufa formations show continuous deposition, while others have little stratigraphic continuity, or show one or more pauses during their deposition. Palaeosols formed in these intervals of paused sedimentation and increased erosion; in pauses in travertine formation, they also reflect increased biological activity and the beginning of weathering (Chafetz and Folk, 1984; Guo and Riding, 1998; Özkul et al., 2002; Faccenna et al., 2008; Van Noten et al., 2018).

The Lake Van Basin plays a key role in Anatolia and the Middle East, as regards tectonism (Şaroğlu and Yılmaz, 1986; Özkaymak et al., 2012; Koçyiğit, 2013; Sağlam Selçuk, 2016; Utkucu et al., 2017; Gülyüz et al., 2019), climate (Landman et al., 1996a, b; Kadıoğlu et al., 1997; Wick et al., 2003; Litt et al., 2011, 2014; Çağatay et al., 2014; Stockhecke et al., 2014; Pickarski et al., 2015), and volcanic and magmatic studies (Zot et al., 2003; Angus et al., 2006; Özacar et al., 2008; Mouralis et al., 2010; Sumita et al., 2012, Sumita and Schimincke, 2013a, b, c; Schmincke and Sumita, 2013; Karaoğlan et al., 2016; Oyan, 2018a; Açlan and Altun, 2018). In this context, understanding travertine formation, an important key to neotectonics in the region, is very important for regional understanding. The Edremit travertines are located east of Lake Van within the Lake Van Basin (Fig. 1A), which developed within a compressional (continent-continental collision) regime starting the Miocene (Şengör and Kidd, 1979; Gülyüz et al., 2019). Eruptions of the Nemrut stratavolcano played an important role in the basin taking its present shape. Özdemir et al. (2006) suggested a 2.5 Ma age for this volcano, and Ulusoy et al. (2012) a 1.01 Ma age. The compressional regime active in the region from 19 Ma, is still effective today and has played an active role in the development of many palaeo- and active faults in the basin (Şaroğlu and Yılmaz, 1986; Özkaymak et al., 2012; Koçyiğit, 2013; Toker, 2013, 2014, 2017b; Utkucu, 2013; Çukur et al., 2014; Erdoğan and Özvan, 2015; Sağlam Selçuk, 2016; Utkucu et al., 2017). These faults may be linked to many travertine deposits in the basin, not least the activity of the Van, Gürpınar and Elmalık faults (Fig. 1B; Yeşilova et al., 2015a, b; Yeşilova, 2019).

The basement of the study area comprises the Paleozoic-Mesozoic Bitlis Massif and the Upper Cretaceous Gevaş Ophiolites (Helvacı et al., 1985). The Van Formation comprising sandstone, claystone, marl and limestone alternations of Burdigalian age unconformably overlies these units (Gülyüz et al., 2019). The succession continues with the Pliocene Kızıltaş Formation consisting of alternations of conglomerate and sandstone (Acarlar, 1991). The Pliocene-Quaternary Büyükçay Formation and Gürpınar Formation unconformably overlie these units. The sequence then ends with the Quaternary Edremit travertines, Van Lake Formation, Gürpınar tufa and finally with lake-stream deposits (Acarlar, 1991; Fig. 1B).

This paper examines the formation and evolution of travertines and tufas in the study area. For this purpose, regional climate, groundwater level, aqueous $CaCO_3$, tectonism, volcanism and magmatic contex will be discussed. In addition, the age of the Van, Gürpınar and Elmalık faults, which are of great importance for regional tectonism and travertine-tufa formation, will be evaluated with respect to the timing of travertine and tufa deposition. This paper is the first detailing travertines/tufas in the Van region which is a “hot spot” for recording Mid to Late Pleistocene and Holocene climate in the Eastern Anatolian highlands, often also used as a major climate reference for understanding climate change in the Eastern Mediterranean.

METHODS

In determining the dynamics (climate, tectonism, volcanism) that play a role in the evolution of travertine and tufa in the Edremit region, field studies (stratigraphic logging, facies analysis) and dating (U/Th) studies have been carried out.

In the field studies, the travertine and tufa deposits were examined in detail from bottom, where they overlie the Van Formation, to top, and a detailed and measured stratigraphic column was prepared to constrain their evolution. To note lateral facies variations, individual layers were followed and section measurements taken at appropriate sites. During the logging, facies analysis and sampling were also carried out. Two different travertine and two different tufa units were observed. From bottom to top these comprise: range-front travertine and bedded travertines (these two travertine units constitute the Edremit travertines); and the Edremit and Çayırbaşı tufas. These units were studied according to their morphological and lithological properties.

Facies were determined by detailed lithological examination (layer location, layer thickness, colour, macrofossil content, macroscopic texture, porosity). Facies associations were determined for each travertine and tufa unit by examining the lateral and vertical continuity of the facies determined. In determining facies, lithological features recorded in previous studies were taken into consideration (e.g., Julia, 1983; Chafetz and Folk, 1984; Pedley, 1990; Ford and Pedley, 1996; Guo and Riding, 1998; Pentecost, 2005; Gandin and Cappezuoli, 2008; Cappezuoli et al., 2014). A complete section was measured from the bottom of the Edremit travertines to the ceiling of the Edremit Tufa. The section was interrupted by three uncompacted units of sandy, silty and clayey, milky brown - brown deposit representing palaeosols (e.g., Kraus, 1999; Retallack, 2014; Tabor and Meyers, 2015), which indicate pauses in sedimentation, used as the determining features in this study (Chafetz and Folk, 1984; Guo and Riding, 1998; Özkul et al., 2002; Faccenna et al., 2008; Van Noten et al., 2018). The carbonate facies were used in palaeoenvironment analysis (cf. Ford and Pedley, 1996; Guo and Riding, 1998; Pentecost, 2005; Cappezuoli et al., 2010).

Minerology-petrography. Forty-two samples were taken for mineralogical and petrographic analysis. Of these samples, 32 were used for thin section analysis, 7 for SEM (Scanning Electron Microscope) and 3 for XRD (X-Ray Diffraction) analysis. XRD samples were taken from the palaeosol levels.

Thin sections. Thin sections of 32 samples were made at Dokuz Eylül University, Torbalý Vocational High School thin section laboratory. Oriented samples were cut into the form of a matchbox. The cut specimens were glued to 2 mm thick frosted glass with araldite and hardener and then thinned using an abrasive disc.

SEM analysis. Seven samples were examined using SEM with EDS (energy-dispersive spectroscopy) at the Scientific Research and Application Center of Van Yüzüncü Yıl University. Natural and polished section samples were coated with Au-Pd

Fig.1A – location map of the study area on a relief map of Turkey; B – geological map of the study area and surroundings

NAF – North Anatolian Fault, EAF – East Anatolian Fault, BSZS – Bitlis-Zagros suture zone; the white arrows indicate the direction of movement of the plates; sample locations are shown by the letter E on the map; all faults on the map are after Koçyiğit (2013); sample coordinates are given on the map

for 90 seconds, examined using a *ZEISS Sigma 300* model SEM microscope and photographed with an SE2 detector.

XRD analysis. XRD analysis was performed on 3 palaeosol samples at the Ankara University Earth Sciences Research and Application Center. One-two g samples were ground in an agate mortar to be under 22 μm, and prepared for analysis to have least orientation, by applying vertical pressure.

U/Th analysis. Sampling began at the contact between the Edremit travertine and the Van formation and continued to each palaeosol level. Then, one sample was taken from below and above each palaeosol level for dating. Samples were taken from the bottom and top levels of the tufas, though not at the palaeosol levels. In addition, sampling was performed systematically from bottom to top. Only one sample was prepared for analysis from the Çayırbaşı tufas. A total of 11 samples were analysed (Table 1).

The samples, of 40–80 g each, were prepared by crushing with a hammer. U/Th analyses were conducted using a

Table 1

Uranium and thorium isotopic compositions and ^{230}Th ages for the travertine and tufa samples

Sample ID	Weight [g]	^{238}U ppb[a]	^{232}Th ppt	$d^{234}U$ measured[a]	$[^{230}Th/^{238}U]$ activity[c]	$^{230}Th/^{232}Th$ atomic (10^{-6})	Age [ka] uncorrected	Age [ka BP] corrected[c,d]	$d^{234}U_{initial}$ corrected[b]
E1	0.0774	353.26 ±0.81	115527 ±875	71.3 ±2.5	1.093 ±0.021	55.1 ±1.1	549 –	542 –	329 –
E2	0.0944	656.4 ±2.1	13591 ±43	64.0 ±3.9	1.1352 ±0.0075	904.0 ±6.0	539 ±63	539 ±62	245 ±97
E3	0.0894	621.5 ±2.0	12868 ±41	60.6 ±3.7	1.0748 ±0.0071	855.9 ±5.7	511 ±92	510 ±92	256 ±101
E4	0.0907	504.50 ±0.88	86344 ±577	89.0 ±2.4	1.109 ±0.014	106.9 ±1.5	474 ±117	470 ±112	336 ±186
E5	0.0752	88.26 ±0.32	1778.3 ±7.6	113.7 ±4.3	1.0674 ±0.0057	873.5 ±5.1	289 ±10	289 ±10	257 ±12
E6	0.0943	510.2 ±1.1	36964 ±195	67.0 ±2.5	0.996 ±0.011	226.7 ±2.7	271 ±13	269 ±13	143.2 ±7.6
E7	0.0884	1700.82 ±3.0	827 ±22	240.4 ±3.2	0.793 ±0.026	26.9 ±1.1	103.1 ±5.1	91.0 ±7.8	301.8 ±7.2
E8	0.0726	4824 ±11	3558 ±189	272.3 ±3.7	0.496 ±0.030	11.1 ±0.89	53.0 ±3.9	34 ±11	296.5 ±8.8
E9	0.0631	4193 ±10	3092 ±164	236.7 ±3.3	0.431 ±0.026	9.64 ±0.78	46.04 ±3431	29.7 ±9.4	257.8 ±7.6
E10	0.0765	525.4 ±1.0	260271 ±3328	894.7 ±4.8	0.213 ±0.012	7.1 ±0.41	12.87 ±0.76	5.7 ±3.7	910 ±11
E11	0.0751	12.772 ±0.060	408.7 ±6.3	246 ±10	0.0319 ±0.0025	16.5 ±1.3	2.83 ±0.22	2.08 ±0.41	247 ±10

Analytical errors are 2 of the mean; [a] – $[^{238}U] = [^{235}U]$ 137.818 (±0.65‰) (Hiess et al., 2012); $d^{234}U = ([^{234}U/^{238}U]_{activity} - 1)$ 1000; [b] – $d^{234}U_{initial}$ corrected was calculated based on ^{230}Th age (T), i.e., $d^{234}U_{initial} = d^{234}U_{measured} X e^{234*T}$, and T is corrected age; [c] – $[^{230}Th/^{238}U]_{activity} = 1 - e^{-l230*T} + (d^{234}U_{measured}/1000)[l_{230}/(l_{230} - l_{234})](1 - e^{-(l230 - l234)*T})$, where T is the age; decay constants are 9.1705 10^{-6} yr^{-1} for ^{230}Th, 2.8221 10^{-6} yr^{-1} for ^{234}U (Cheng et al., 2013), and 1.55125 10^{-10} yr^{-1} for ^{238}U (Jaffey et al., 1971); [d] – age corrections, relative to 1950 AD, were calculated using an estimated atomic $^{230}Th/^{232}Th$ ratio of 4 (±2) 10^{-6}; those are the values for a material at secular equilibrium, with the crustal $^{232}Th/^{238}U$ value of 3.8; the errors are arbitrarily assumed to be 50%

multi-collector inductively coupled plasma mass spectrometer (MC-ICP-MS), Thermo Electron Neptune, at the High-precision Mass Spectrometry and Environment Change Laboratory (HISPEC), Department of Geosciences, National Taiwan University. A triple-spike ^{229}Th-^{233}U-^{236}U, isotope dilution method (Shen et al., 2003) was used to correct for instrumental fractionation and to determine U/Th isotopic and concentration (Shen et al., 2012). The half-lives of U-Th nuclides used are available in Cheng et al. (2013). Uncertainties in the U-Th isotopic data and ^{230}Th dates are calculated at the 2 level or two standard deviations of the mean (2 $_m$) unless otherwise stated.

RESULTS

SEDIMENTOLOGY AND PALAEOGEOGRAPHY

In the field, the travertines and tufas were examined vertically and laterally and a generalized column section was prepared representing them (Fig. 2). In logging, the layers were followed laterally so that a complete section could be constructed (Fig. 2). The travertines and tufas in the study area were divided into four: range-front travertines which formed between 542.4–538.7 ka; stratified travertines which formed between 538.7–29.7 ka; the Eremit tufas which formed between 30–5.7 ka; and the Çaırbaşı tufas which formed at 2.1 ka (Fig. 2).

Range-front travertines. These basal travertines are medium to thick bedded with a total thickness of 3 m (Fig. 3A, B). They contain angular blocks of Van Formation sandstone and siltstone 30–70 cm across (Fig. 3B) and round burgundy-red pebbles also from the Van formation. The travertines are milky pink-brown in colour. All the range-front travertines are of pebbly facies (Figs. 3B and 4A). They were observed at the boundary of the Edremit travertines with the Van Formation, at its eastern border where Van Fault passes.

Layer-type travertines. Beige-cream coloured, rarely grey, travertines with an average thickness of 145 m are bedded, varying from laminated to thick bedded. Lamina thicknesses vary between 5–8 mm, and bed thicknesses between 1 and 80 cm. The formation of these travertines, which conformably overlie the range-front travertines, continued for 504.6 ky.

Field studies determined a total of 6 lithofacies in the Edremit travertines: crystalline crust facies, reed-type facies, shrub-type facies, lithoclast-breccia facies, paper-thin raft-type facies and palaeosol facies. The bedded travertines begin with crystalline crust facies at the base and end in shrub-type facies at the top.

Crystalline crust facies. This facies, milky coffee-cream-beige coloured, is one of the most commonly encountered and dominant facies in the study area (Fig. 2). With layer thicknesses varying from 0.8 to 60 cm, the facies has a hard and compact structure (Figs. 3B and 4B).

Reed-type facies; This light to dark brown facies is thinnest and least widely distributed in the study area, mostly being associated with shrub-type facies. It includes remnants of reeds and sedge, in places perpendicular to the base, but mostly distributed randomly through the layers (Fig. 4C, D). Layer thickness varies from 1–5 cm. The facies outcrops on the south slope of the travertines in the study area and in low-slope areas between Çayırbaşı village and Edremit county.

Shrub-type facies. This grey-light brown facies is observed most often horizontally and vertically in the study area, and mostly contains gas cavities (Fig. 4D). In the field, it is usually found together with paper-thin raft and reed-type facies. Bed thicknesses varies from 10 to 30 cm. It outcrops beneath the Edremit tufa in the study area (in the southeast) and around Edremit county. This facies mostly outcrops in areas where the slope flattens.

Lithoclast-breccia facies. This cream-beige and occasionally brown facies has bed thicknesses varying from 40–120 cm. It was observed at three separate levels along the measured stratigraphic section, generally developing above palaeosol fa-

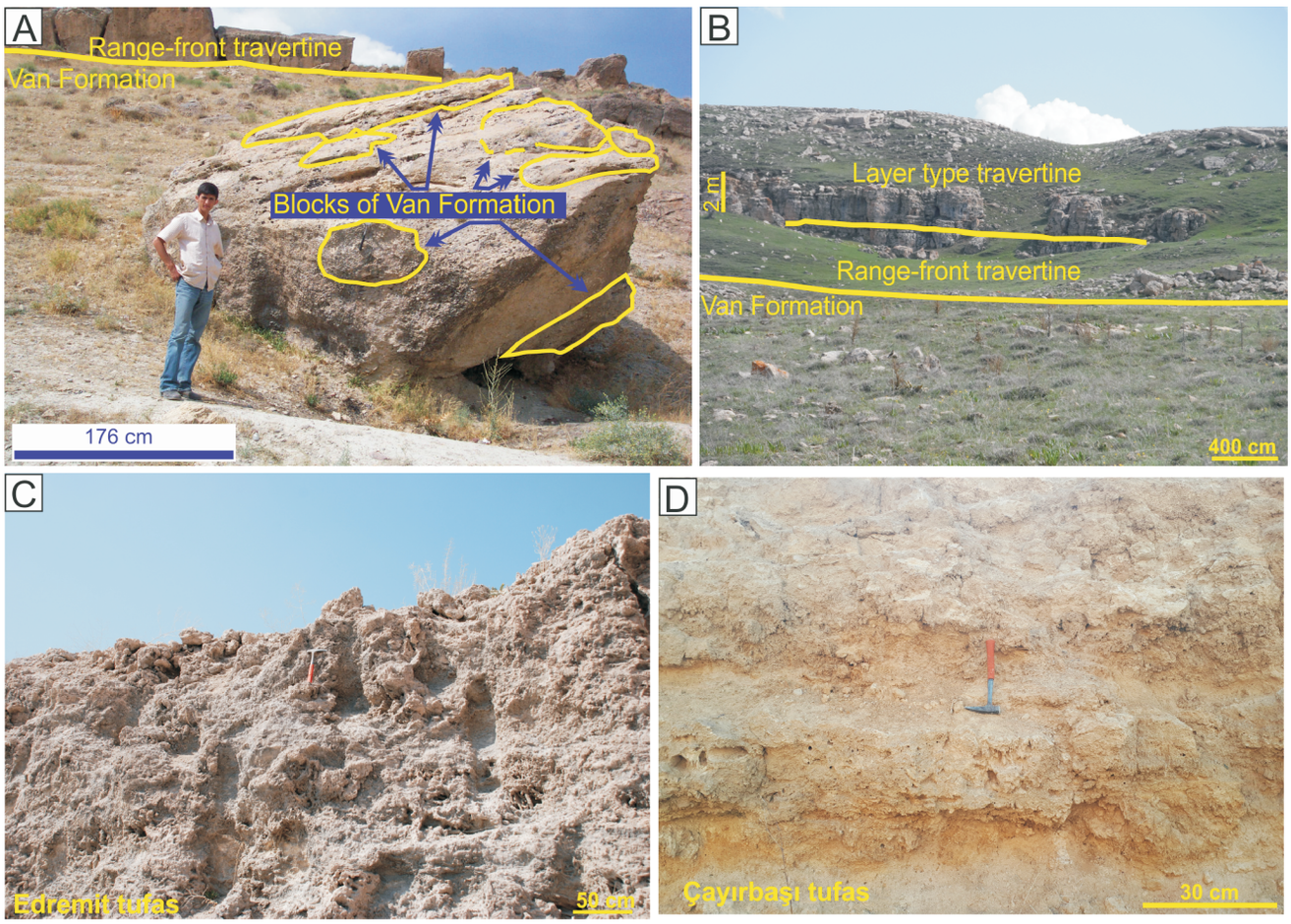

Fig. 2A – range-front travertine, which forms the base of the Edremit travertines; B – pictures of Van formation exposures: Range-front travertine, Layer type travertine; C – Edremit tufas; D – Çayırbaşı tufas

cies (see Fig. 2). It comprises angular and poorly-sorted travertine pebbles (4–114 mm across) in a binding carbonate mud (Fig. 4E). It was observed north of Köprüler village and south of Elmalık village.

Paper-thin raft-type facies. Layer thicknesses varies from 1–15 mm. These thinly laminted deposits appear like single thick layers due to calcite mud plastering the surroundings (Fig. 4F). In the study area this grey-light brown facies outcrops in flat areas between Çayırbaşı village and Edremit county and was the third most commonly observed facies.

Palaeosol facies. Formed during degradation. weathering and transport of the travertines, this facies is light to dark brown. While the palaeosols examined in the region overlie the travertines with an irregular surface, sharply bounded travertines overlie them in turn. A 2 m thick palaeosol accumulated over a 20 ky time interval between 289–269 ka, while the other two palaeosols have thicknesses of 50–100 cm (Fig. 4G, H). These thicknesses decrease downslope. This facies was observed southwest of Elmalık village, in the 3rd km along the Edremit–Gevaş highway and east of Köprüler village.

Edremit tufa. Tufas precipitated between 29.7–5.7 ka are light brown-yellow, and consist of stromatolites and phytoclastic tufa. Tufa nearly 30 m thick outcrops in an area between the travertines in the study area and the shore of Lake Van (west-south-west of the travertines).

The phytoclast tufa facies was formed by cementing large and small plant remains – mostly sedge-reed type plants – and leaves with carbonate (Fig. 5A). The plant remains are variously dispersed, form a clast-supported fabric, and are well-cemented (Fig. 5A).

The stromatolite tufa facies was observed in limited areas on the coast of Lake Van, comprising stromatolites 20–70 cm long and 5-15 cm thick. The facies – whose lower and upper boundaries are made of clear white coloured sparry calcite (Fig. 5B) – are laterally and vertically transitional into phytoclast tufa facies.

Çayırbaşı tufa. These formed before 2.08 ka in a small lake on the Edremit travertines. This dark to light brown tufa comprises plants and leaf fragments and phytoclasts within a micritic tufa facies consisting of carbonate mud layers. Leaf fragments were observed in the lowest levels of the tufa (Fig. 5C). In the upper levels, fragments of reed, but no leaf fossils, were observed. Nearly 2 m thick overall, bed thickness varies from 2–45 cm (Fig. 5C, D).

The phytoclast tufa facies is dark to light brown with bed thicknesses varying from 5–45 cm (Fig. 5C), consisting of weakly cemented, fragile plant stems and leaves (Fig. 5D). The micritic tufa facies is dark to light brown, the carbonate mud and layers varying from 2–15 cm (Fig. 5C) and alternating with the phytoclast tufa facies (Fig. 5C). No other sedimentary structures were observed.

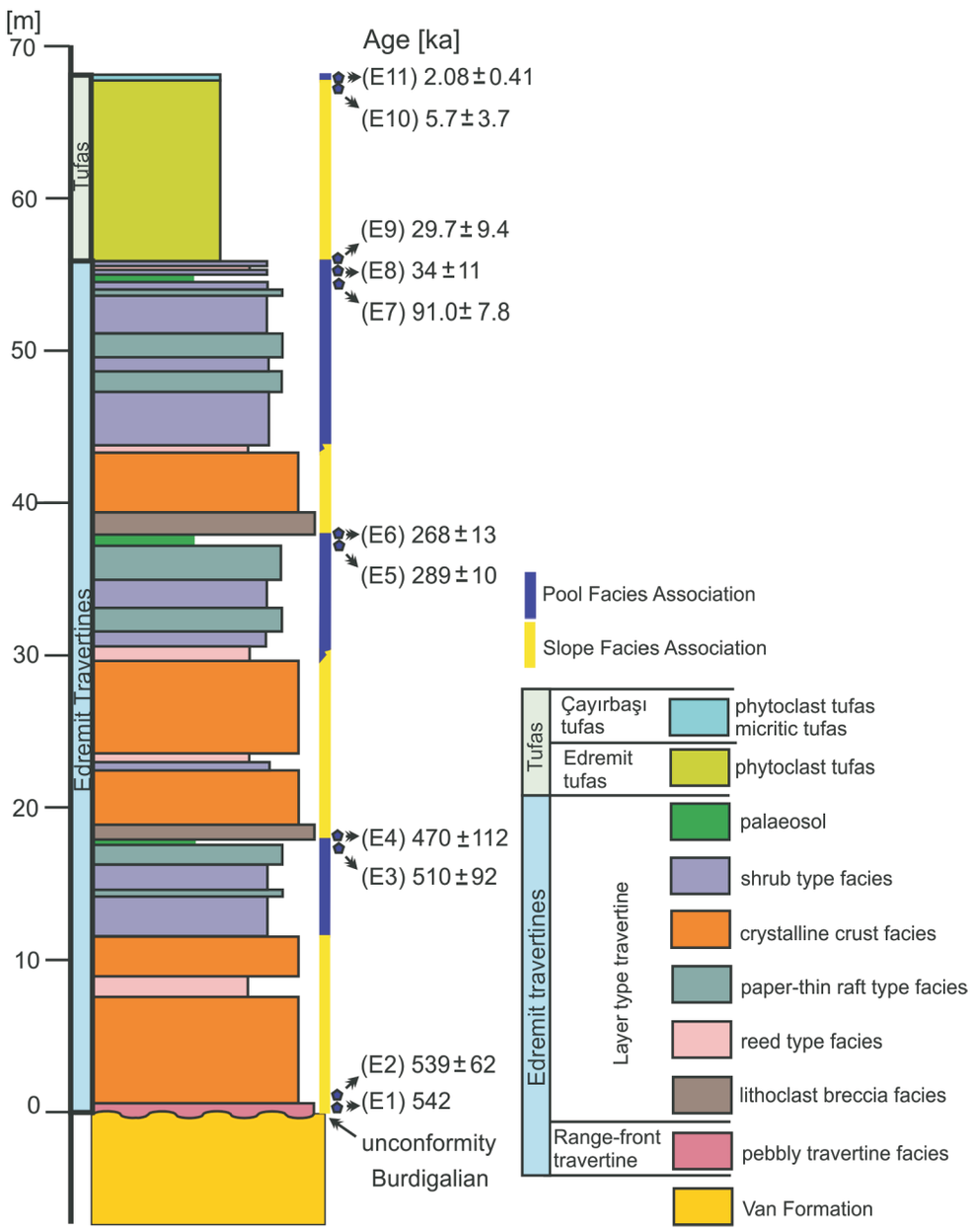

Fig. 3. Log section showing travertine and tufa in the Edremit region

In the cross-section, facies associations and sample locations are also shown

MINERALOGY AND PETROGRAPHY

The crystalline calcite facies is composed of calcite crystal bundles perpendicular to the depositional surface (Fig. 6A, B). The upper surfaces of the crystal bundles consist of fans with conchoidal structure (Fig. 6B). Calcite crystals have developed in smoothly and compactly without leaving any space between them (Fig. 6C). In thin section, crystalline shells show thin lamination and layers of calcite cutting the crystals perpendicular to their elongation (Fig. 6A). These thin laminations are growth lines that are convex upwards and develop from the fan base upwards (Fig. 6B). In thin section, calcite crystals forming the crystal fans show broad extinction patterns under cross-polarized light (Fig. 6A). However, radial fans developing in tandem are approximately equal in length (Fig. 6B).

The lithoclasts forming the lithoclast-breccia facies consists of grains eroded from the travertine. Ooid grains are sparsely encountered within the facies (Fig. 6D). Clasts derived from the crystalline crustal facies form the grains in the cores of the ooids (Fig. 6D). The clasts are surrounded by clear sparry calcite (Fig. 6D). These concentric sparry calcite rings are occasionally accompanied by micritic calcite.

The shrub-type facies was observed in the sections examined as arborescent-shrub growths formed by branches spreading from more than one leaf. When longitudinally cut sections of the leaves are examined, ooid-like structures are observed (Fig. 6E), consisting of micritic carbonate (Fig. 6E). In the middle of these structures are calcite crystals and around them are decayed bacterial cells (Fig. 6F). SEM analyses of the bacterial remains indicate abundant microporosity of the micritic leaves (Fig. 6E, F).

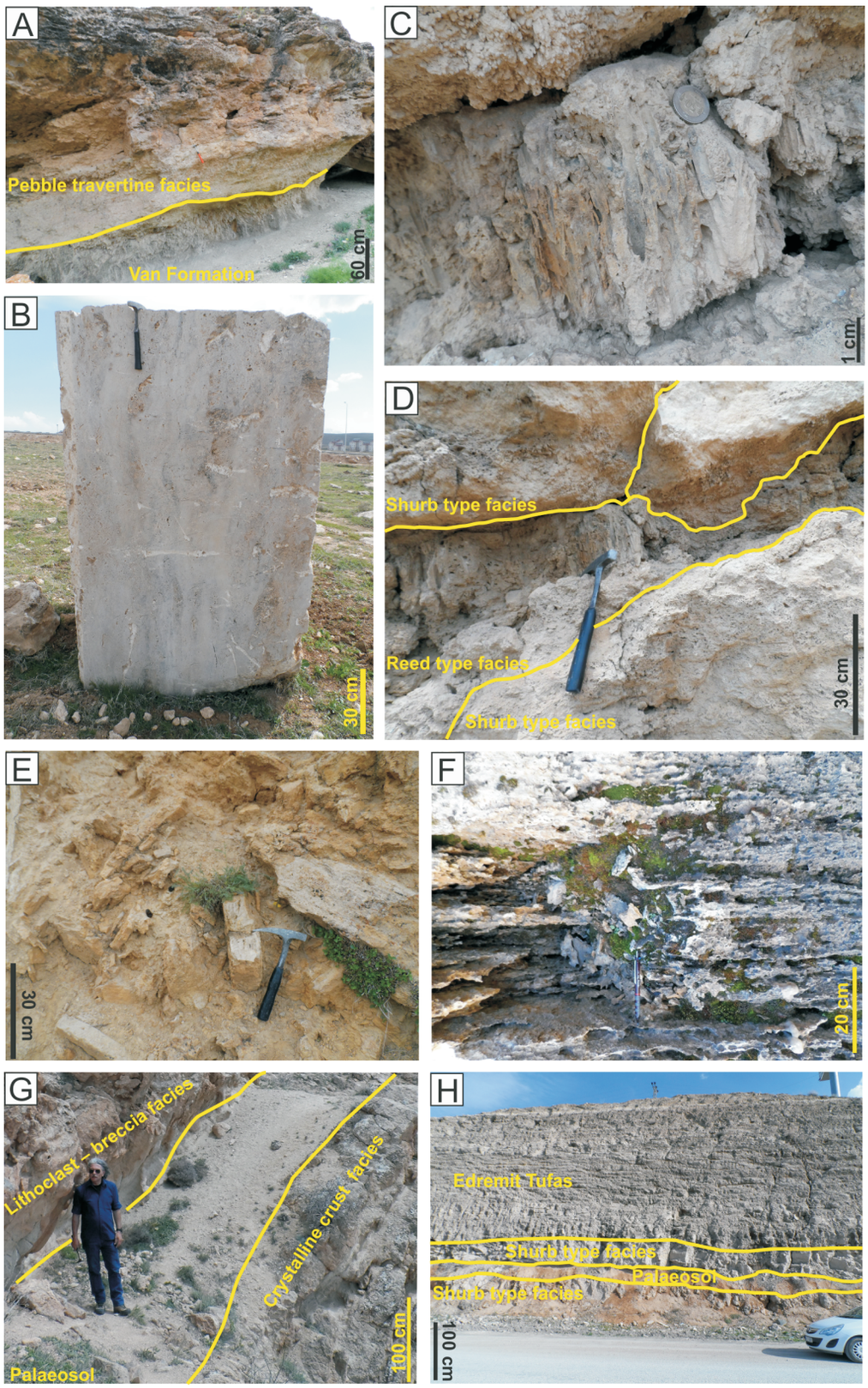

Fig. 4A – relation between pebble travertine facies and the Van Formation; B – crystalline crust facies; C – reed type facies; D – shrub type and reed type facies association; E – lithoclast-breccia facies; F – paper-thin raft facies; G – lithoclast-breccia facies, palaeosol and crystalline crust facies; H – Edremit tufa at the top, shrub type facies, palaeosol and again shrub type facies below

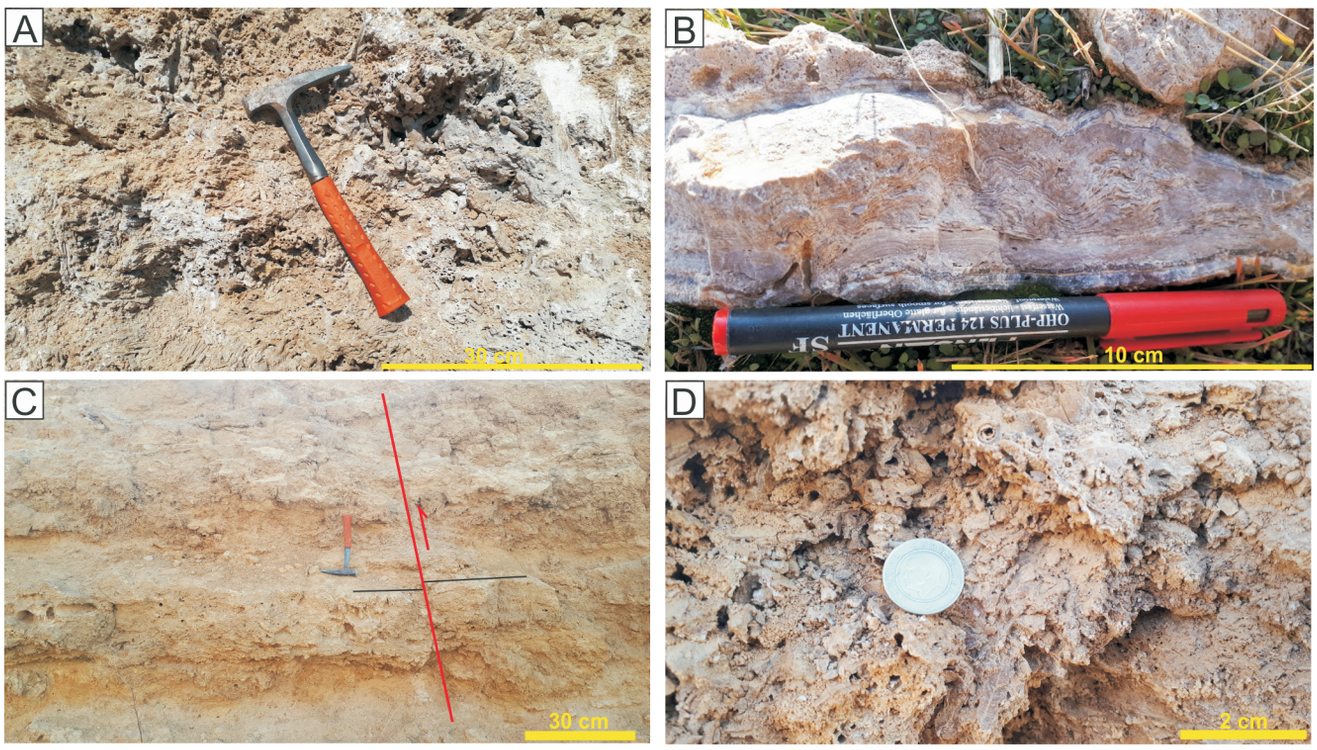

Fig. 5A – Edremit tufas containing abundant plant stems and leaf fragments; B – stromatolites observed in coastal areas of Lake Van; C – Çayırbaşı tufas consisting of alternations of phytoclast tufa facies and micritic tufa facies; D – phytoclast tufa

The stromatolite tufas are composed of thin laminae (Fig. 6G). The upper surfaces of the stromatolites are overlain by 5–9 mm thick sparry calcite laminae (Fig. 6H, I), with microbial mats between the calcite laminae (Fig. 6J).

The phytoclast tufa facies is formed by the cementing of plant branches, roots and leaf parts with calcite. In SEM analysis of crystalline samples, rim-structured calcite filaments developed to fill the spaces between calcite crystals are seen (Fig. 6K). In samples with micritic structure, microbial mats with occasional cyanobacterial filaments are observed on calcite crystals (Fig. 6L).

In the XRD analysis of samples taken from 3 palaeosol facies in the study area, clay, carbonate, quartz, gypsum and plagioclase peaks are present (Fig. 7), with quartz and kaolin being predominant. Chlorite, vermiculite and smectite with a peak value of 14.3760 Å and illite with a peak value of 9.8402 Å were detected (Fig. 7A). Dolomite and plagioclase were only found in palaeosol 2 (Fig. 7B) with a peak values of 3.1620 Å and 2.9750 Å respectively, and also clay minerals at 17.2761 Å and 5.4984 Å peak values and anhydrite with a 3.5565 Å peak value (Fig. 7B). In palaeosol sample 3, gypsum with a peak value of 7.5126 Å was observed, with gypsum at 3.0649 Å peak accompanied by calcite (Fig. 7C).

DISCUSSION

INTERPRETATION OF FACIES ASSEMBLAGES

Travertine facies can be used to interpret such factors as distance from source, depositional environment, interruptions in deposition and fault/fracture activity (Kitano, 1963; Chafetz and Folk, 1984; Folk et al., 1985; Chafetz et al., 1991; Ford and Pedley, 1996; Guo and Ridding, 1998; Özkul et al., 2002). Each facies observed in the study area represents different depositional environments, water temperatures and tectonic activity/inactivity.

Considering features of the depositional environment (formation temperature, slope, mineralogical and petrographic properties, plant content/biological activity and aqueous regime) and lithotypes of travertine facies in the study area (Guo and Riding, 1998; Özkul et al., 2014), two different facies associations were investigated (see Fig. 2), namely slope and pool facies associations. In determining the slope facies association, parameters such as the temperature of the water, the slope of the layers and the biological activity were taken into consideration (e.g., Guo and Riding, 1998; Özkul et al., 2014; Cappezuoli et al., 2014). In determining the pool facies association, parameters such as the horizontality of the layers forming the facies, layer thickness, type of cement (micrite/sparite) and the high biological activity were taken into account (e.g., Guo and Riding, 1998; Özkul et al., 2014; Cappezuoli et al., 2014).

Slope facies association. This facies association will be discussed separately for the Edremit travertines and Edremit tufas.

Edremit travertine. The slope facies association is commonly characterized by crystalline crust facies (see Fig. 2), which may be accompanied by reed-type facies and lithoclast-breccia facies. These types of facies association generally form on slopes with dips varying from 7 to 35°. This facies association is observed above nearly every palaeosol facies. Crystalline crust facies development indicates a relatively hotter water source (e.g., Guo and Riding, 1998). This facies association develops with limited biological activity due to rapid water

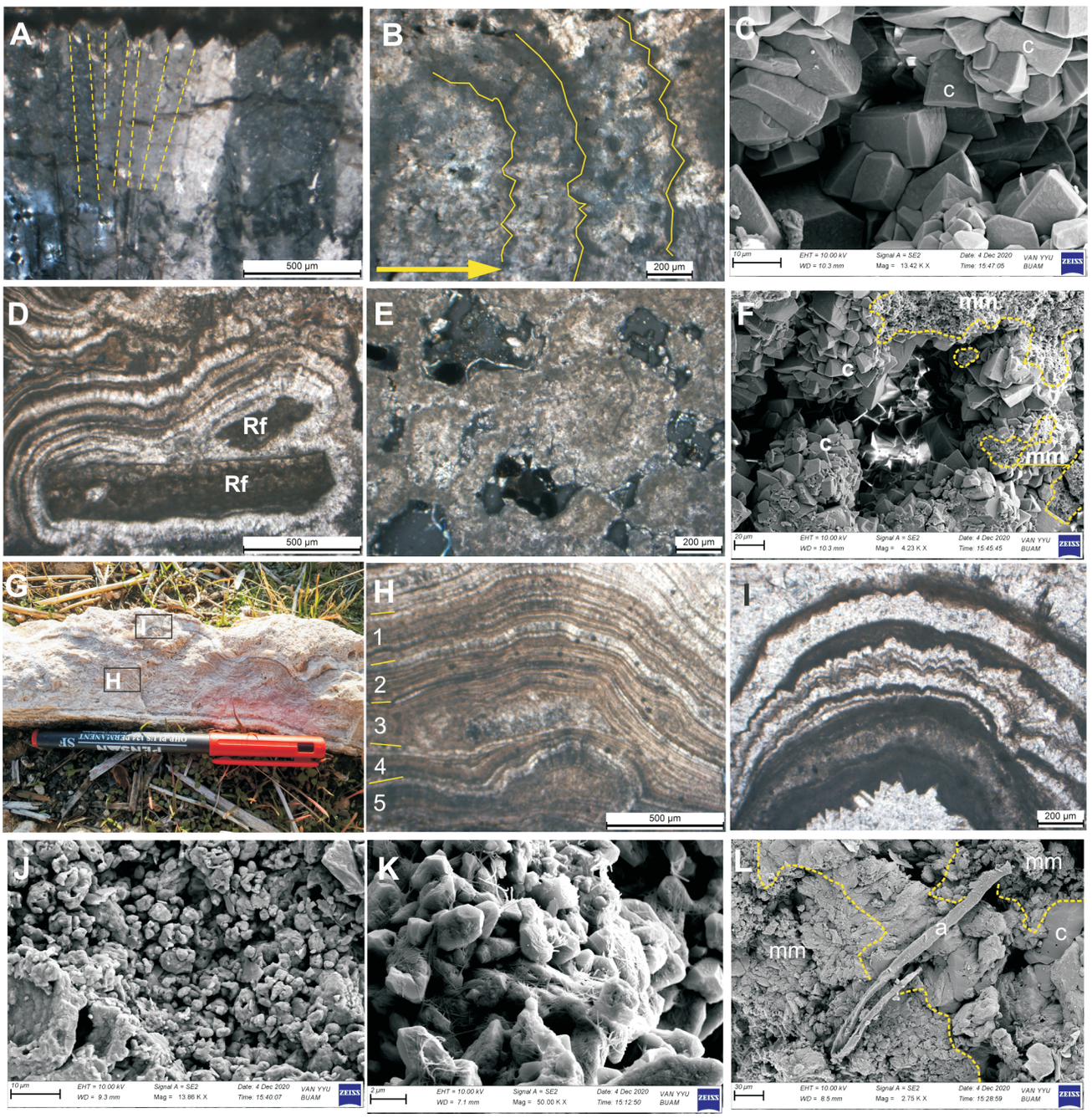

Fig. 6. Thin-section and SEM images of Edremit travertine and tufa

A – calcite crystal that develops perpendicular to the plane of the bed; **B** – crystalline crustal facies with upward growth; **C** – calcite crystals (c); **D** – Calcite grain (Rf) and its surrounding concentric calcite growths; **E** – shrub-type facies; **F** – cavity structure in shrub-type facies with calcite crystals (c) and decayed bacteria (mm); **G** – photo showing the transverse and longitudinal development of stromatolites; **H–J** – thin section images of stromatolite (H and I) and microbial mat in between (J); **K** – lattice bladed structured calcite filaments; **L** – cyanobacteria filament (a) and microbial mat (mm); A, B, E, H – crossed polars, D and I – plane polarized light

flow (Guo and Riding, 1998). Thin and long crystalline calcite bundles perpendicular to the depositional surface observed in thin section support this inference (see Fig. 6A, B; e.g., Barilaro et al., 2011). Also, the ray-crystal fans being equal and in length and of the same growth rate indicates that stable ambient conditions and water flow rate (see Fig. 6C; e.g., Özkul et al. 2001; Barilaro et al., 2011). Concentric clear calcite rings (see Fig. 6D) that make up the ooids indicate rapid flow. All these features show that these facies were deposited on a the hillside. However, the reed-type facies indicates lower water temperatures and renewed biological activity (Guo and Riding, 1998) and it shows similar characteristics to tufa. Cappezuoli et al. (2014) called such reed type travertines 'travitufa'. This facies association, repeated 5 times in the study area, can be inferred to form from hot waters on slopes (e.g., Guo and Riding, 1998; Özkul et al., 2014; Cappezuoli et al., 2104).

Edremit tufas. Phytoclastic tufa occurs within this facies association. These tufas are grain-supported, calcite-ce-

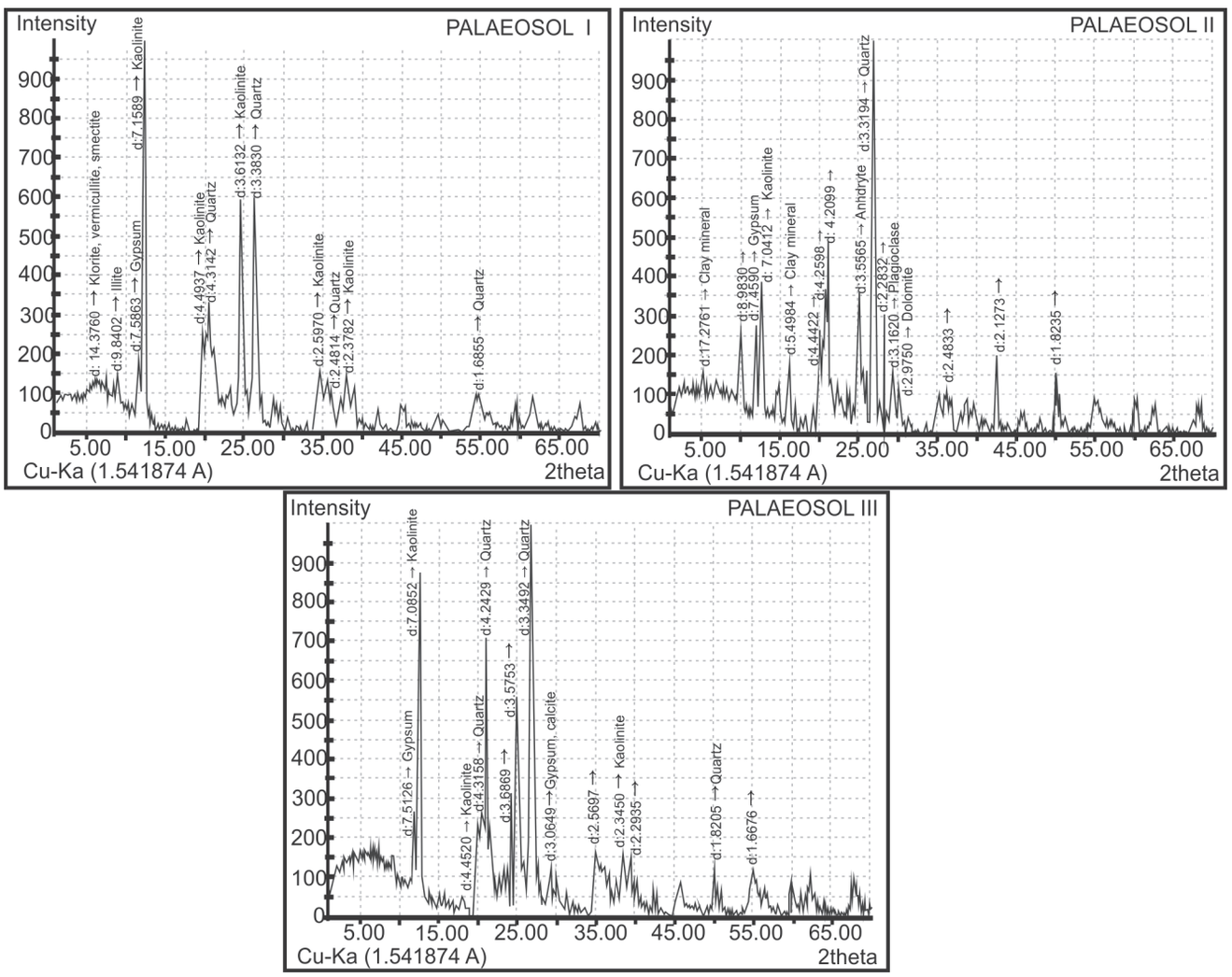

Fig. 7. X-ray diffraction analysis of palaeosols

Results of palaeosol I, palaeosol II and palaeosol III analyses

mented, highly porous, and contain abundant plant stems and leaf fragments. The microbial mats and cyanobacteria filament observed in the SEM images indicate viable microbial activity during tufa precipitation (see Fig. 6L; Özkul et al., 2002; Tlili et al., 2021), though the cyanobacteria filament may, by its location, be a product of environmental contamination. The calcite filaments in cross-section show the connection of organic with physico-chemical precipitation (see Fig. 6K; Tlili et al., 2021). These tufas have been investigated within the slope facies association because they are inclined (17–30°), formed on slopes and do not show lacustrine features (terraces, lacustrine sediment; e.g., Pedley, 1990; Glover and Robertson, 2003; Cappezuoli et al., 2014). Cold mineral waters emerging from the spring (Elmalık Fault) allowed abundant plant formation, and the waters flowing down the slope formed the Edremit tufas.

Pool facies association. This facies association will be discussed separately for the Edremit travertines and Çayırbaşı tufas.

Edremit travertine. This facies association consists of facies deposited in horizontal or near-horizontal areas where the slope flattens out (Guo and Riding, 1998), and comprises shrub-type and paper-thin raft type facies (Fig. 3), associated with reed-type and slope facies. Özkul et al. (2014) investigated the palaeosol facies within this facies association, characterized by changes in the fluid regime (amount and flow direction), reduction and/or cessation of travertine-forming flow, and linked to increased biological activity (e.g., Chafetz and Folk, 1984; Guo and Riding, 1998; Özkul et al., 2002; Faccenna et al., 2008). In general this facies association is associated with lake environments rather than lithological features (Guo and Riding, 1998). The facies typically occurs above the slope facies association in transition to reed-type facies and shows a fall in water temperature, a change from a sloping to a horizontal setting and the development of lacustrine areas. The bushes observed in thin sections and SEM images consist of carbonate mud, contain organic components, and were deposited horizontally in superposition, showing that they formed in a lake/pool environment with slow water flow (see Fig. 6E, F; Barilaro et al., 2011; Chafetz, 2013).

Edremit tufas. Stromatolite of this facies association have been studied in restricted areas along the shore of Lake Van. Lake level has been shown to have risen up to 1720 m a.s.l. (Kuzucuoğlu et al., 2010; Yeţilova et al., 2019), but no stromatolites have been found at 1660 m a.s.l. and above, as any tufa surfaces are covered by dense vegetation and/or forms a settlement area. The stromatolites investigated stromatolites are compatible with the thin planar stromatolites

that Martin-Bello et al. (2019) named Ls.1. These are characterized by flat or slightly wavy laminae at the bottom, and are domed upwards (see Fig. 6G), showing that the lake water level rose over time (Martin-Bello et al., 2019). In thin section, upper stromatolite surfaces consist of clear calcite, indicating wave/current activity (see Fig. 6G, H, I; e.g., Martin-Bello et al., 2019). High biological activity was observed in SEM images (see Fig. 6K). Yeşilova et al. (2019) stated that the lake level was at the same level as today at 30 ka and that it had risen rapidly after this time. The age of formation of these stromatolites (Edremit tufas), which are observed at an average height of 1660 m a.s.l., is consistent with this data, as are the lake water levels shown by the domes in the upper parts of the stromatolites (Yeşilova et al., 2019).

Çayırbaşı tufas. This horizontally bedded tufa represents a lacustrine environment of micritic tufa facies (see Figs. 1 and 5E, F), representing the pool facies association (e.g., Chafetz and Folk, 1984; Guo and Riding, 1998; Özkul et al., 2002; Faccenna et al., 2008; Cappezuoli et al., 2014). However, considering both their elevation (2100 m a.s.l.) and their formation time (between 5.7–2.08 ka), the environment in which they were formed was a seasonal lake conducive to travertine formation. An altitude of 2100 m a.s.l. has not been previously indicated for Lake Van, and so the, Çayırbaşı tufas were formed in a local lacustrine area fed by surface waters. The presence of these tufas only in a certain area, not overlying all of the travertines, supports this inference.

Yeşilova et al. (2019) stated that while the water level of Lake Van was 1704 m a.s.l. at 112.7 ka, the lake level at 30.1 ka (1646 m.a.s.l.) reflects the recent lake level. This study shows that the water level of the lake rise rapidly after this period, reaching 1723 m a.s.l. at 19.3 ka, and subsequently 1725.2 m a.s.l. Kuzucuoğlu et al. (2010), in their study of the Van Lake terraces, stated that, based on lacustrine deposits in Engil Stream, the water level of Lake Van rise to 1725 m a.s.l. and that the water level of Lake Van was 1755 m a.s.l. at 115 ka, one of the highest values measured. In this context, based on previous studies, lacustrine sediments or interactions should have been seen in the travertine and tufa of the region. However, in our investigations, no lacustrine influence was found in the travertines. However, stromatolites have been found only in a limited part of Edremit tufas, being observed only in very limited areas where vegetation is sparse in the coastal areas of Lake Van, at up to 1660 m a.s.l., not being found at higher elevations. There are several possible explanations: (i) There may have been no lacustrine sediment accumulation on the travertines, or the lacustrine sediments may have been eroded by lake level fluctuations, (ii) lacustrine action (terrace / sediment) may have been present on the travertines, but settlements and orchards are widespread at elevations of 1800 m a.s.l. and below, hindering examination. (iii) The topography may have been too sloping to permit the formation of travertine or tufa within the lake. The lacustrine tufa occurrences mostly occur at streams or water outlets, or beaches where there is no slope (this situation is expressed for Lake Van; e.g., Yeşilova et al., 2019). As the Edremit beach of Lake Van has a steep slope and there are permanent settlements at 1800 m a.s.l. and below, lacustrine inputs (terraces / sediments) were not observed in the travertine or tufa.

Range-front travertines under the layer-type travertines reflect tectonic activity, including fault movement, in the region at 542 ka and/or before (e.g., Barnes et al., 1978; Ayaz, 2002). With faults being active in the region before 542 ka, hot and mineralized water began to form the basal part of the range-front travertines (e.g., Barnes et al., 1978; Ayaz, 2002), limestone and marbles (Bitlis Massif and Gevaş Ophiolite) likely being the source of the calcium enrichment in these waters. Layer-type travertines formed in the 538.7–29.7 ka interval were deposited on these travertines. It is possible to recognize that these travertine depositional episodes occurred as 3 separate stages punctuated by palaeosol facies. The base of each of these three separate travertine units occurring from 539–91.0 ka begins with the slope facies association and ends with the pool facies association (Fig. 3). This situation shows that as sedimentation continued, the sloping surfaces approached a horizontal attitude and the environment transformed into a lacustrine setting. This also indicates that the temperature of hot mineral waters was gradually decreasing (e.g., Chafetz et al., 1991; Ford and Pedley, 1996; Guo and Ridding, 1998; Özkul et al., 2002). The palaeosol facies ending these 3 separate travertine depositional episodes occurred at 3 different times: 510–470 ka, 289–269 ka, and 91.0–34 ka (Figs. 3 and 8). This situation indicates cessation/source changes in the water forming the travertines and, as a result, pauses in travertine formation (Chafetz and Folk, 1984; Guo and Riding, 1998; Özkul et al., 2002, 2010; Faccenna et al., 2008). The reason for the tectonic instability occurring in these time intervals may be blockage of fractures by the $CaCO_3$ precipitated from groundwater, preventing water reaching the surface. In the interval from 34–30 ka, facies characterized by lacustrine environments were again deposited (Fig. 3). However, the Edremit travertines transformed into tufa developments from 29.7 ka. Edremit tufas have been precipitated from this time until 5.8 ka, composed of reed-sedge plants (Fig. 2A) and oak tree remains (Fig. 2C) (e.g., Pedley, 1990; Glover and Robertson, 2003). Above these tufas, the Çayırbaşı tufa continued to develop until 2.08 ka, again characterized by a lacustrine environment (e.g., Pedley, 1990; Glover and Robertson, 2003). The Çayırbaşı tufas only crop out in a local lacustrine area (~2 km^2).

FACTORS CONTROLLING TRAVERTINE AND TUFA FORMATION

Travertine and tufa formation are controlled by many factors, notably tectonism, climate and volcanism, that determine the source and amount of water, calcium content, morphology and biological activity (Julia, 1983; Barnes et al., 1978; Chafetz and Folk, 1984; Pedley, 1990; Altunel and Hancock, 1993a, b; Ford and Pedley, 1996; Guo and Riding, 1998; Pentecost, 2005; D'Alessandro et al., 2007; Huybers and Langmuir, 2009; Guido et al., 2010; Cappezuoli et al., 2014). In this study, the faults (Aydan et al., 2011; Kartal et al., 2012; Koçyiğit, 2013; Sağlam Selçuk, 2016) controlling the formation and development of the travertine and tufa were studied, and climatic parameters with reference to previous studies (Lisiecki and Raymo, 2005; North Greenland Ice Core Project members, 2004; Steffensen et al., 2008; Svensson et al., 2008; Wolff et al., 2010; Barker et al., 2011). Volcanism and magmatism in the region were also evaluated in the light of previous studies (Keskin, 2003; Zot et al., 2003; Angus et al., 2006; Özacar et al., 2008, Özdemir and Güleç, 2014; Kidd et al., 2015; Oyan et al., 2016, 2017; Karaoğlan et al., 2016; Açlan and Altun, 2018; Oyan, 2018a, b). The waters forming the travertine and tufa around Lake Van also feed and influence the chemistry of Lake Van. Therefore, there is a clear relationship between the previous chemical studies carried out in Lake Van and the waters forming the travertines. The formation of the Edremit travertine is nearly equivalent (with appropriate error bars) to the formation of Lake Van. In a sense, Lake Van may play a key role in explaining the evolution of the travertines in many respects, such as climate, level changes, calcium carbonate chemistry,

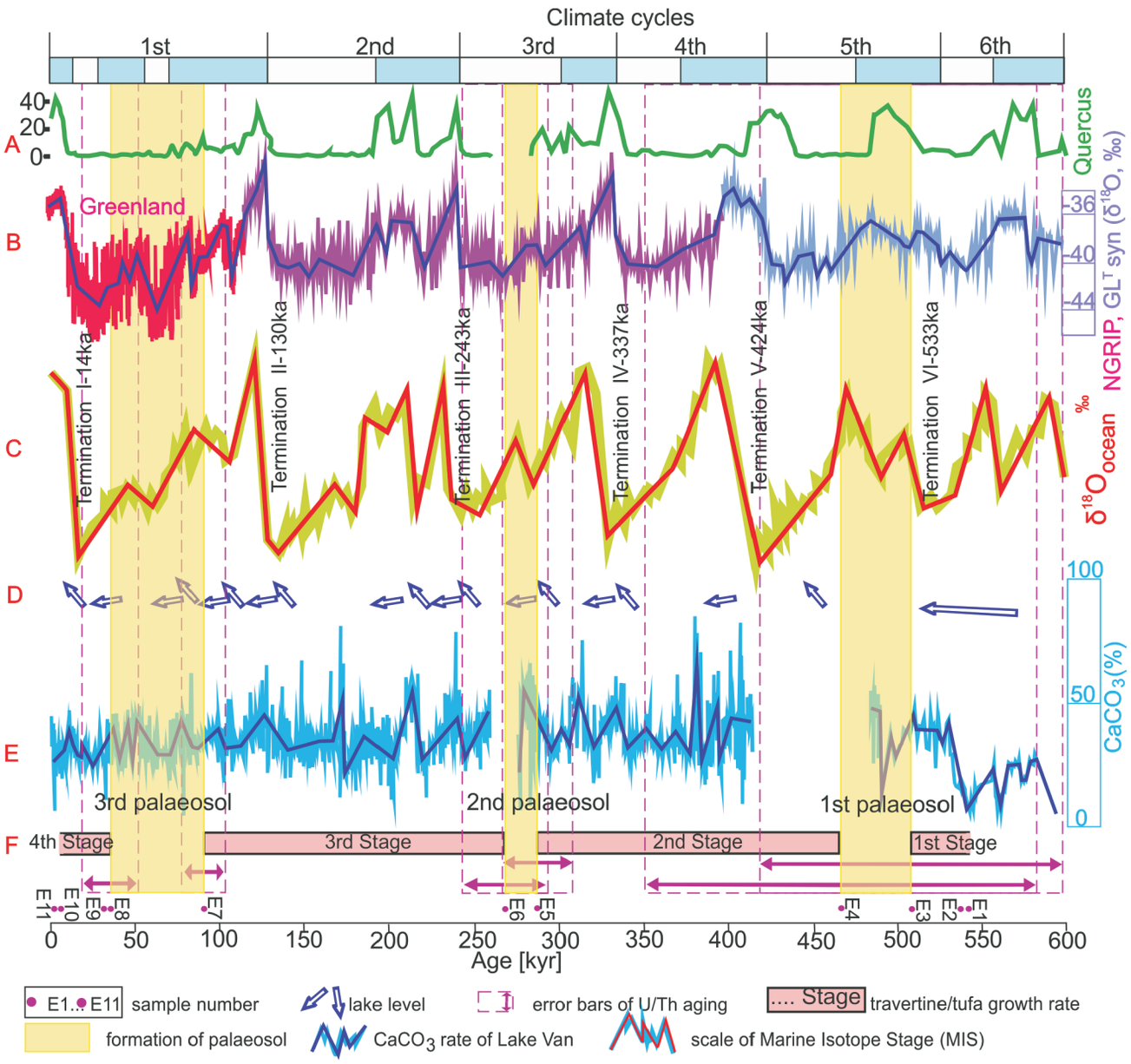

Fig. 8. Comparison of Edremit travertine formation with marine stratigraphy of Lisiecki and Raymo (2005), which includes 6 glacier-interglacial alternations. Lake Van Quercus pollen by Litt et al. (2014)

Marine Isotope Stage (MIS) (stack of 57 globally distributed benthic ^{18}O records); NGRIP/GLT-syn and ^{18}O values (North Greenland Ice Core Project members, 2004; Steffensen et al., 2008; Svensson et al., 2008; Wolff et al., 2010; Barker et al., 2011); Van Lake level changes (Stockhecke et al., 2014) and $CaCO_3$ values (Stockhecke et al., 2014) are shown by yellow box, pauses (palaeosol) and error bars (purple arrows and dashed lines) in the precipitation of the Edremit travertines; the pink bars show the travertine/tufa development stages; at the same time, the palaeosol times and development stages are correlated with all these components

tectonism, volcanism and magmatic context. Through the action of different faults continuing to be active in the region currently, tectonism plays a key role in illuminating the evolution of the Edremit travertines and tufas.

Climate. The travertines and tufas deposited around Edremit reflect 3 pauses/repetitions (3 separate palaeosol formations; Fig. 8). Stockhecke et al. (2014) examined the 600,000-year-old sedimentary evolution of Lake Van and correlated it the study of Lisiecki and Raymo (2005) based on a stack of benthic marine ^{18}O records. They found that the Van Lake history was coeval with more than 6 glacial/interglacial alternations on the scale of Lisiecki and Raymo (2005). When the palaeosol dates are correlated with the marine isotope record of Lisiecki and Raymo (2005), the 1st palaeosol development appears to be equivalent to the glacial phase of the 5th cycle, the 2nd palaeosol is equivalent to the interglacial of the 3rd cycle and the 3rd palaeosol is equivalent to one glacial and one interglacial phase of the 1st cycle (Fig. 8). The palaeoclimate in the Lake Van basin has been studied via the record of *Quercus* pollen in the lake sediments by Litt et al. (2014). Comparing the pollen data of this study to the palaeosols in the Edremit travertines, the 3rd and 2nd palaeosol formations are compatible with the pollen data, while the 1st palaeosol formation is incompatible. This situation may be explained by the wide error bars constraining the palaeosol formation time (Fig. 8). Correlations with regional climate databases (NGRIP/GLT-syn ^{18}O) (North Greenland Ice Core Project members, 2004; Steffensen et al., 2008; Svensson et al., 2008; Wolff et al., 2010; Barker et

al., 2011) show that the 1st palaeosol is equivalent to times of rising temperature, while the 2nd and 3rd palaeosols are equivalent to times when temperature fell (Fig. 8). In general, it was found that palaeosol formation times were relatively more consistent with the MIS scale (Fig. 8). In the correlation, it was determined that the 3rd and 2nd palaeosol times coincide with glacial phases (after Termination I and after Termination III), and the 1st formation time (before Termination VI) coincides with a warm phase. Palaeosol developments have thus not been detected for every glacial phase, although in general they coincide with glacials (Fig. 8; Tabor and Meyers, 2015).

In the XRD data, chlorite and quartz, which reflect arid and cold environments, were found in all palaeosol samples (see Fig. 7; e.g., Singer et al., 1994; Southard and Miller, 1996; Tabor and Meyers, 2015). However, these components are common in all detrital and immature palaeosols and are not a stand-alone indicator of climate (Southard and Miller, 1996; Thomas et al., 2011; Tabor and Meyers, 2015). The anhydrite, plagioclase and dolomite observed in the 2nd palaeosol sample show that deposition occurred in dry and cold climatic conditions (see Fig. 7B; Sheldon and Tabor, 2009; Babechuk and Kamber 2013; Tabor and Meyers, 2015). In the 3rd palaeosol sample, chlorite, illite and smectite accompanying kaolinite and quartz indicate dry and cold climate conditions (see Fig. 7A) (Banfield and Murakami, 1981). However, the presence of gypsum and calcite accompanying kaolinite and quartz in the 1st palaeosol sample also points to arid climatic conditions as well as a relatively mild climate (according to palaeosol I and palaeosol II; see Fig. 7C; Sheldon and Tabor, 2009; Tabor and Meyers, 2015). Comparison of all the XRD results obtained with the palaeosol formation times and the climate at that time, indicates that the data are mutually compatible. In this case, the formation times of the 3rd and 2nd palaeosol indicate cold and arid climates, while the time of the 1st palaeosol formation indicates dry but hot climate conditions. All these data are compatible with the graph in Figure 8.

In addition, many studies related to climate have been conducted in the study area and its immediate surroundings (Djamali et al., 2008, 2012; Litt et al., 2009; Stevens et al., 2012; Yeşilova et al., 2019; Ön and Özeren 2019). These studies covered the period from the 3rd travertine growth stage to the present. The third palaeosol coincides with the last glacial phase (e.g., Tzedakis, 1994; Akçar and Schlüchter, 2005; Djamali et al., 2008; Pickarski et al., 2015).

Considering these results, it appears that climate change has a small influence on the formation of the Edremit travertine and a large influence on the Edremit and Çayırbaşı tufas.

Fluctuations in lake level and $CaCO_3$ contents. A study of the 600,000-year sedimentary evolution of Lake Van by Stockhecke et al. (2014) identified fluctuations in lake level and variations in the $CaCO_3$ levels in the lake. Variations in lake level are important controls on groundwater levels and variations in $CaCO_3$ levels are directly associated with $CaCO_3$ levels in sources feeding the lake. Therefore, an increase or decrease in the carbonate content in the streams feeding Lake Van increases or decreases the amount of carbonate in the lake. Likewise, the rise or fall in lake level causes the groundwater level in the lake basin to rise or fall. Considering the travertine and tufa formation and cessation periods around Edremit, during each palaeosol formation a fall in the $CaCO_3$ level of the lake was observed (Stockhecke et al., 2014). However, cessation of travertine formation was not observed with each decrease in lake $CaCO_3$ level. The same study observed that level variations in Lake Van were not directly correlated to travertine formation (Stockhecke et al., 2014) and that by contrast with many fluctuations in lake level, only 3 cessations were observed in the travertines. Hence, fluctuations in level or $CaCO_3$ in the lake (Stockhecke et al., 2014) were not associated with travertine formation.

In these interpretations, the error bars in the U/Th dating of palaeosol formation (especially the very large error bar for 1st palaeosol formation) should be considered (Fig. 8).

Tectonism. Travertine deposition is directly associated with active faults (Barnes et al., 1978) that transport hydrothermal fluids to the surface (Sibson et al., 1975). The majority of travertines studied have formed and continue to form from the Pleistocene to the present day around the world (Schwarcz and Latham, 1984; Chafetz and Folk, 1984; Goff and Shevenell, 1987; Kronfeld et al., 1988; Heimann and Sass, 1989; Pentecost and Tortora, 1989; Altunel and Hancock, 1996; Guo and Riding, 1998; Özkul et al., 2002, 2010, 2013, 2014; Faccenna et al., 2008; Mesci et al., 2008, 2013; Mohajjel and Taghipour, 2014; Brogi et al., 2016; Alçiçek et al., 2017; Henchiri et al., 2017). The tectonic disturbance of travertine deposits may be used to characterize the palaeoseismic activity of active faults (Martinez-Diaz and Hernández-Enrile, 2001; Gradziński et al., 2014). As a result, the neotectonic regime has an important role in explaining tectonism at the present day (Altunel, 1996; Martinez-Diaz and Hernández-Enrile, 2001; Gradziński et al., 2014; Giustini et al., 2018).

Many faults in the study area played a direct role in the evolution of the travertine and tufa deposits. These include the normal Van Fault and the reverse Gürpınar Fault (Koçyiğit, 2013; Sağlam Selçuk, 2016), involved in the development of the Edremit travertines, and the left-lateral strike-slip Elmalık Fault (Koçyiğit, 2013) playing an active role in development of the Edremit tufas.

The Van Fault, 24 km long, striking NW and with a normal slip component, shapes the Van Lake shore (Koçyiğit, 2013). The range-front travertine formation developed along this fault line shows that this fault was the source of water issuing to form the Edremit travertine (e.g., Barnes et al., 1978; Altunel and Hancock, 1993a, b; Ayaz, 2002). The Van Fault, which has no data on wheni it formed, was most recently active on 9 November 2011 (Aydan et al., 2011; Kartal et al., 2012). However, as travertine formation occurred due to activity on this fault (Fig. 1C), the fault must have formed at 542 ka or before. With weak climate control, formation of the Edremit travertine was apparently controlled by tectonism. The Edremit travertine is also important in showing periods when travertine formation stopped (palaeosol facies formation) and erosion began. As a result, cessations in travertine formation indicate cessations in tectonic activity (Chafetz and Folk, 1984; Guo and Riding, 1998; Özkul et al., 2002; Faccenna et al., 2008). From the formation times of palaeosol in the Edremit travertine, it is inferred that the Van Fault was active every 180 ky (with error bars), and then had periods of inactivity for ~40 ky (with error bars; Fig. 9). Considering this situation, the currently active (Aydan et al., 2011; Kartal et al., 2012) Van Fault will be active for another ~146 ky in the future (Fig. 9).

Another fault controlling the development of the Edremit travertine is the E–W striking Gürpınar Fault, with a total length of 78 km (Koçyiğit, 2013; Sağlam Selçuk, 2016). With no data about its age, the Güzelsu segment of the fault is known to have produced an earthquake on 7 April 1964 (Ambraseys and Jackson, 1998). Currently still active, the fault has a 0.5 mm/yr^{-1} slip rate (Sağlam Selçuk, 2016). Affecting the south edge of the Edremit travertine and tufa, it played an active role in shaping this edge. Controlling the south of the Van Fault, the formation age of the Gürpınar Fault should be younger than the Van Fault. As a result, the age of this fault must be younger than 542 ka.

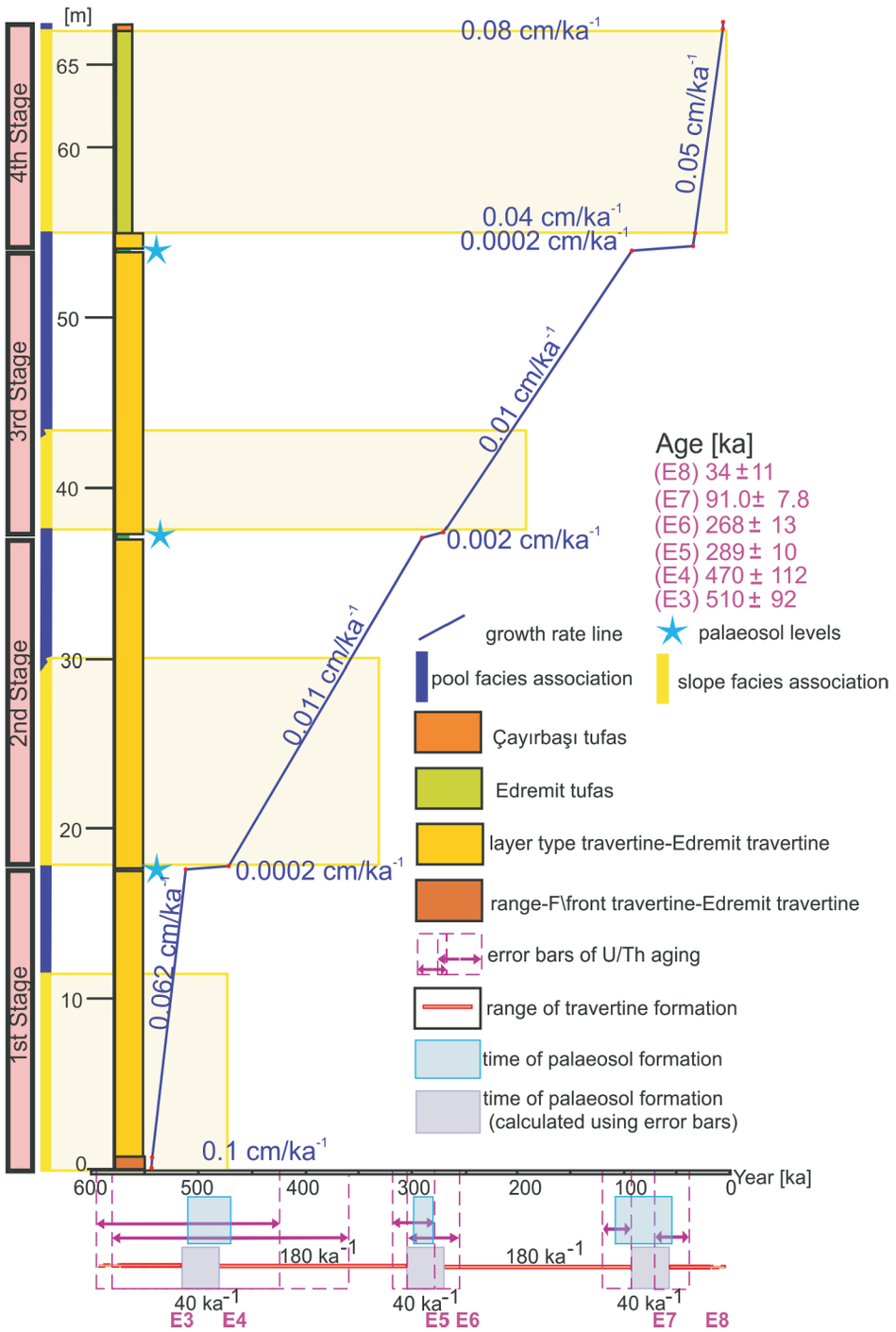

Fig. 9. Stage of growth charts of travertine and tufa around Edremit area

Purple boxes and age ranges of palaeosols with error bars have been adapted by us

With a mean length of 10 km, the Elmalık Fault has NE strike and is a left-lateral strike-slip fault (Koçyiğit, 2013). The Edremit travertine is cut by this fault showing the age of the fault is younger than the travertine deposition. Again, it was identified that this fault controlled the Edremit tufa (if it did not, tufa should be observed in the western section of the travertines). In this context, the age of the fault should be equivalent to the age of the tufa formation (29.7 ka), consistent with the Edremit tufa not being observed in the regions above the Elmalık Fault, which is located 150 m below the Van Fault. As this fault developed, the source of the water that formed the travertines also changed. As the spring-fed water started to form the Edremit tufa at lower elevations, deposition of the Edremit travertines ceased. Thus, the Van Fault has been active from 34 ka until today, but does not now form travertine. Observation of the uppermost levels of the tufa shows that activity continued until 5.7 ka. The current tufa formation and the dense vegetation in some areas in the Edremit region indicate that the Elmalık Fault and spring water are still active, while dense human settlement and orchard development in these areas hindered tufa deposition (e.g., Goudie et al., 1993; Nyssen et al., 2004).

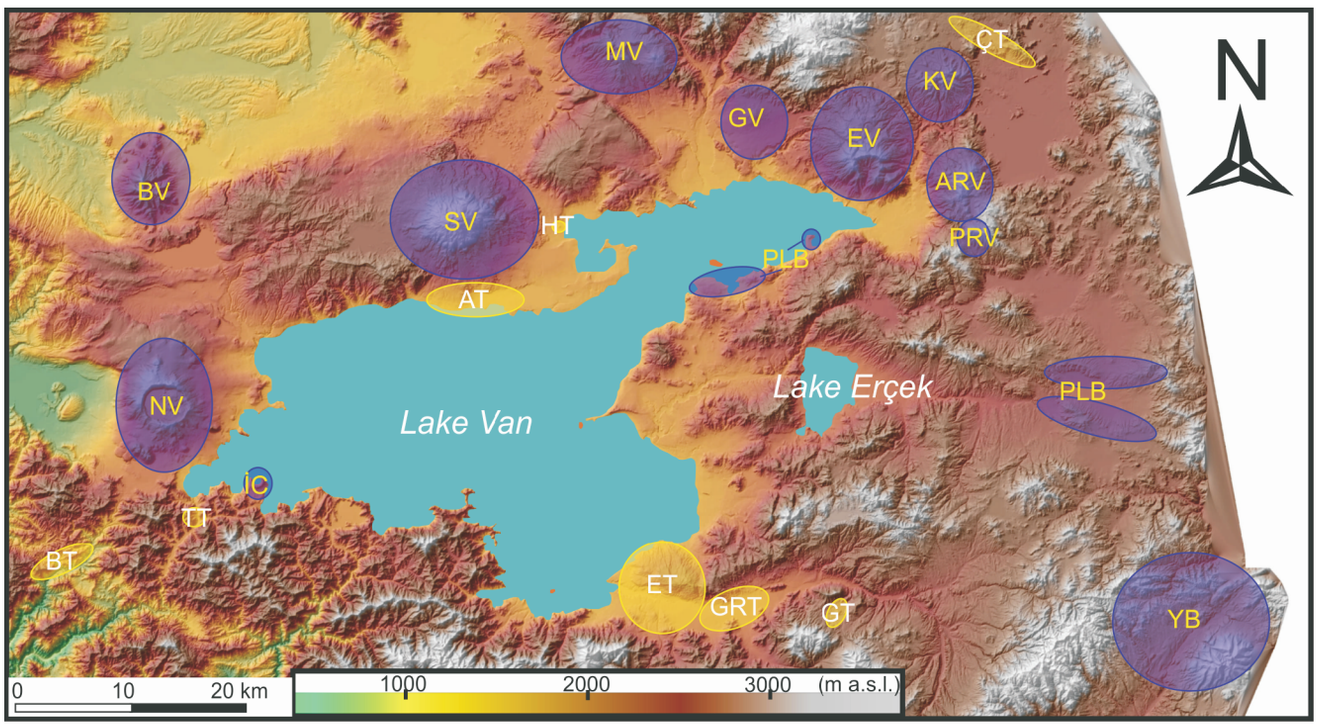

Fig. 10. Relief map showing volcanism-magmatism and travertine and tufa deposits around Lake Van

NV – Nemrut volcano; BV – Bilican volcano; SV – Süphan volcano; MV – Meydan volcano (caldera); GV – Girekol volcano; EV – Etrüsk volcano; PRV – Pirres¸it volcano; ARV – Argıt volcano; KV – Kösedag volcano; PLB – Pliocene basalts; YB – Yavuzlar basalts; BT – Bitlis travertine; TT – Tatvan travertine; AT – Adilcevaz tufa; HT – Heybeli travertine; ET – Edremit travertine and tufa; GRT – Gürpınar tufa; GT – Gürpınar travertine; detailed information about the Miocene and the Pliocene volcanic units was given by Oyan et al. (2016)

Volcanism and magmatic contex. Volcanic activity in the Lake Van basin located in the Eastern Anatolian High Plateau started after continental collision in the Miocene. It started just north of Lake Van 15 Ma (Lebedev et al., 2010) and continued until 1441 CE (Özdemir et al., 2006). The youngest volcanism identified in the region took place on the northern part of Nemrut Volcano in 1441 (Özdemir et al., 2006). This volcanic activity, which covers approximately half of the Van Lake basin, took place both along opening fractures and from large volcanic centres such as Nemrut, Süphan, Tendürek, Ağrý, Meydan, Etruscan and Girekol. Recent studies indicate that the last oceanic lithosphere in the Eastern Anatolian region was completely exhausted 20 Ma (Okay et al. 2010), while collision likely was in the Late Oligocene–Early Miocene (25–30 Ma) (Karaoğlan et al., 2016; Oyan, 2018a; Açlan and Altun, 2018). Geophysical studies conducted in the region indicate that the lithospheric mantle is very thin and the crust varies in thickness between 38-45 km (Zot et al., 2003; Angus et al., 2006; Özacar et al., 2008; Kidd et al., 2015). This situation resulted in a shallow asthenosphere and the development of intense magmatic activity with melting in both the asthenospheric mantle and the lithospheric mantle (Keskin, 2003; Özdemir and Güleç, 2014; Oyan et al., 2016, 2017; Oyan, 2018b). The very thin lithosphere and the shallow setting of the asthenospheric mantle indicate the rise of hot mantle below the zone and indicate that melting continued throughout the Quaternary with a steep theremal gradient below the zone (Oyan et al., 2016, 2017; Oyan, 2018b). These events are interpreted as the main reason for the warming of the ground waters and the thermal activity in the region. These thermal waters played a role in the occurrence of travertines that formed in the region from the Pleistocene. At the same time, the CO_2 released into the atmosphere by volcanism may have affected the climate and triggered the ending of glacial phases (Huybers and Langmuir, 2009). It also contributed to the formation of carbonates via dissolution in high-CO_2 hydrothermal fluids released to the surface (D'Alessandro et al., 2007; Guido et al., 2010; Cappezuoli et al., 2014; Giustini et al., 2018), resulting in the travertine sedimentation in the region during the Quaternary (Fig. 10).

Stage of growth of travertine/tufa. Growth rates of tufa and travertines are controlled by many factors such as stream/groundwater chemistry, vegetation type, topography, biotic-abiotic mechanisms, climate and tectonism (Gradziński, 2010; Capezzuoli et al., 2014). The growth rate for tufa is between 0–5 cm/ky^{-1} (Weijermars et al., 1986; Heiman and Sass, 1989; Andrews et al., 2000) and for travertine, it averages 20 cm/ky^{-1} (Pentecost, 2005). The travertine and tufa in the region grew in 4 stages (see Fig. 8). Stage 1 is the travertine deposition which took place between 542 and 510 ka at a rate of 0.1–0.062 cm/ky^{-1} (Fig. 9). Stage 2 is the precipitation of travertine at a rate of 0.011 cm/ky^{-1}, between 470 and 289 ka (Fig. 9). Stage 3 is the travertine deposition at a rate of 0.01 cm/ky^{-1}, between 268–91 ka (Fig. 9). The fourth and final stage is tufa-travertine precipitation, which took place between 34–2.08 ka at an average of 0.05 cm/ky^{-1} (Fig. 9). These growth rates of travertine and tufa show values below the rates described in previous studies. However, the error bars of the calculated ages are large (especially 470 ka and later) and erosion prevailed in the region for an average of 40 ky after each travertine depositional episode (Fig. 9). These two factors are thought to be the main reasons for these apparent low growth rates. In addition, fluctuating climate during deposition may also have influenced the low growth rates (see Fig. 8). Even during the last stage (average 0.05 cm/ky^{-1}) with small error bars, low erosion and a rela-

tively warm climate is relatively warm, the growth rate is below average, suggesting a low $CaCO_3$ concentration in the groundwater. However, it was observed that the slope of the layer decreases towards the upper parts of the travertines. A system develops in which the upward slopes decrease with continuous deposition on the sloping travertines at the slope base (e.g., Luo et al., 2021). This sedimentation system eventually passes into maturity (Luo et al., 2021). Due to calcium deficiency, it is consumed quickly in the proximal region and the products are limited. Due to the long gaps that develop in front of the slopes, collapsed travertine deposits or unidentified hiatus develop in these areas (Gradzinski et al., 2018). Low growth rates in travertine and tufa in the region are thought to be related to such unidentified hiatuses (e.g., Gradzinski et al., 2018).

The data described above (climate, volcanism, tectonism, lake fluctuations and lake $CaCO_3$ concentrations) show that the pause periods (palaeosol facies) in the Edremit travertines coincided with the periods when the Van Fault was not active. However, no palaeosol facies has been encountered in the developmental stages of tufa, the formation of which took place under climate control.

CONCLUSIONS

Climate, volcanism and teconism are interpreted as the main factors influencing the travertine and tufa deposits observed in the Edremit region. Tectonism was effective in the shaping and development of the travertines, while climate shaped the development of the tufa. Growth rate graphs (Figs. 8 and 9) of the travertines and tufas indicate that the maximum rates correspond to specific climate phases (e.g., 539–510 ka and 30–5.7 ka).

Three main faults and two different water sources played an important role in the formation and current geometry of the travertines and tufas; (i) the Van fault associated with formation of the Edremit travertines, (ii) the Gürpınar Fault associated with the geometry of the Edremit travertines, and (iii) the Elmalık Fault associated with the formation of the Edremit tufas. Water sources were: (i) the source formed by the effect of Van Fault, forming the Edremit travertines; and (ii) the source exposed by the Elmalık Fault and forming the Edremit tufa.

U/Th ages from the Edremit travertines indicate a 542 ka depositional age for the travertines, therefore the minumum age of the Van fault is constrained as 542 ka.

The Gürpınar Fault played a role on the formation of travertine deposition along the southern margin of the Edremit travertines and affected the current geometry of the Van fault. In this respect, the maximum age of the fault is constrained as 542 ka (or younger). Movement on the fault, field observations and the geometry of the travertines might have been associated with uplift by Gürpınar Fault activity. Further tectonic studies are needed to constrain such an uplift/offset mechanism and to calculate an uplift rate.

The Elmalık Fault affected the formation of the Edremit tufas. In this regard the minumum age of the fault is constrained as 29.7 ka.

The growth pattern of the Edremit travertines indicates three breaks and erosional (palaeosol) intervals during deposition. These intervals correspont to 510–470 ka, 289–269 ka and 91.0–34 ka. These palaeosol intervals can be considered as evidence for inactive periods of the Van fault since they are direct evidence of cessation in sedimentation solely associated with the fault activity. By considering the active (around 180 ky with error bars) and inactive (around 40 ky with error bars) periods of the fault, it might be suggested that the currently active Van faults will be active for the following 146 ky since the youngest palaeosol formation age is 34 ka.

Acknowledgements. We are grateful to M. Gradziński, C. Helvacı, S. Üner and E. Gülyüz for their help in writing and evaluating this paper. This study was supported by Y. Yıl University Scientific Research Project Council (YYÜ, BAP, Project No: 2014-MİM-B074). U/Th dating was supported by grants from the Science Vanguard Research Program of the Ministry of Science and Technology (MOST) (108-2119-M-002-012 to C.-C.S.), the National Taiwan University (109L8926 to C.-C.S.), the Higher Education Sprout Project of the Ministry of Education, Taiwan ROC (108L901001 to C.-C.S.).

REFERENCES

Acarlar, M., Bilgin, A.Z., Elibol, E., Erkan, T., Gedik, I., Guner, E., Hakyemez, Y., Şen, A.M., Uğuz, M.F., Umut, M., 1991. Van Gölü doğusu ve kuzeyinin jeolojisi (in Turkish). MTA Report No. 9469, Ankara.

Açlan, M., Altun, Y., 2018. Syn-collisional I-type Esenköy Pluton (Eastern Anatolia-Turkey): an indication for collision between Arabian and Eurasian plates. Journal of African Earth Sciences, **142**: 1–11.

Akçar, N., Schlüchter, C., 2005. Paleoglaciations in Anatolia: a schematic review and first results. Eiszeitalter und Gegenwart, **55:** 102–121.

Alcicek, M.C., Alcicek, H., Altunel, E., Arenas, C., Bons, P., Brogi, A., Capezzuoli, E., de Riese, T., Della Porta, G., Gandin, A., Guo, L., Jones, B., Karabacak, V., Kershaw, S., Liotta, D., Mindszenty, A., Pedley, M., Ronchi, P., Swennen, R., Temiz, U., 2017. Comment on "First records of syn-diagenetic non-tectonic folding in Quaternary thermogene travertines caused by hydrothermal incremental veining" by Billi et al. Tectonophysics, **721**: 491–500.

Altunel, E., 1996. Morphological features, ages and neotectonic importance of the Pamukkale travertines (in Turkish with English summary). Bulletin of Mineral Research and Exploration Institute (MTA) of Turkey, **118**: 47–64.

Altunel, E., Hancock, P.L., 1993a. Morphology and structural setting of Quaternary Travertines at Pamukkale, Turkey. Geological Journal, **28**: 335–346.

Altunel, E., Hancock, P.L., 1993b. Active fissuring faulting in Quaternary travertines at Pamukkale, western Turkey. Zeitschrift für Geomorphologie Supplement-Band, **94**: 285–302.

Altunel, E., Hancock, P.L., 1996. Structural attributes of travertine filled extensional fissures in the Pamukkale plateau, Western Turkey. International Geology Review, **38**: 768–777.

Ambraseys, N.N., Jackson, J.A., 1998. Faulting associated with historical and recent earthquakes in the eastern Mediterranean region. Geophysical Journal International, **133**: 390–406.

Andrews, J.E., 2006. Palaeoclimatic records from stable isotopes in riverine tufas; synthesis and review. Earth-Science Reviews, **75**: 85–104.

Angus, D.A., Wilson, D.C., Sandvol, E., Ni, J.F., 2006. Lithospheric structure of the Arabian and Eurasian collision zone in Eastern Turkey from S-wave receiver functions. Geophysical Journal International, **166**: 1335–1346.

Ayaz, M.E., 2002. Travertenlerde gözlenen morfolojik yapılar ve tabiat varlığı olarak önemleri (in Turkish). Cumhuriyet Üniversitesi Yerbilimleri, **19**: 123–134.

Aydan, O., Ulusay, R., Kumbasar, H., Konagai, K., 2012. Site Investigation and Engineering Evaluation of the Van Earthquakes of October 23 and November 9, 2011. Technical Report. Japan Society of Civil Engineers (JSCE).

Barilaro, F., Della Porta, G., Ripamonti, M., Capezzuoli, E., 2011. Petrographic and facies analysis of Pleistocene travertines in Southern Tuscany, Central Italy. AAPG Search and Discovery Article. 90124. 2011 AAPG Annual Convention and Exhibition, April 10–13, 2011, Houston, Texas.

Barker, S., Knorr, G., Edwards, L., Parrenin, F., Putnam, A.E., Skinner, L.C., Wolff, E., Ziegler, M., 2011. 800,000 years of abrupt climate variability. Science, **334**: 347.

Barnes, L., Irwin, W.P., White, D.E., 1978. Global distribution of carbon dioxide discharges, and major zones of seismicity. U.S. Geological Survey, Water-Resources Investigations, Open-File Report, **78–39**.

Brogi, A., Liotta, D., Meccheri, M., Fabbrini, L., 2010b. Transtensional shear zones controlling volcanic eruptions: the Middle Pleistocene Mt. Amiata volcano (inner Northern Apennines, Italy). Terra Nova, **22**: 137–146.

Brogi, A., Alçiçek, M.C., Yalçıner, C.C., Capezzuoli, E., Liotta, D., Meccheri, M., Rimondi, V., Ruggieri, G., Gandin, A., Boschi, C., Büyüksarac, A., Alçiçek, H., Bülbül, A., Baykara, M.O., Shen, C.-C., 2016. Hydrothermal fluids circulation and travertine deposition in an active tectonic setting: insights from the Kamara geothermal area (western Anatolia, Turkey). Tectonophysics, **680**: 211–232.

Capezzuoli, E., Gandin, A., Sandrelli, F., 2010. Calcareous tufa as indicators of climatic variability: a case from the Southern Tuscany (Italy). Geological Society Special Publications, **336**: 263–281.

Capezzuoli, E., Gandin, A., Pedley, M., 2014. Decoding tufa and travertine (fresh water carbonates) in the sedimentary record: The state of the art. Sedimentology, **61**: 1–21.

Chafetz, H.S., Folk, R.L., 1984. Travertines: depositional morphology and the bacterially constructed constituents. Journal of Sedimentary Petrology, **54**: 289–316.

Chafetz, H.S., Rush, P.F., Utech, N.M., 1991. Microenvironmental controls on mineralogy and habit of $CaCO_3$ precipitates: an example from an active travertine system. Sedimentology, **38**: 107–126.

Cheng, H., Edwards, L.R., Shen, C.C., Polyak, V.J., Asmerom, Y., Woodhead, J., Hellstrom, J., Wang, Y., Kong, X., Spotl, C., Wang, X., Calvin, A.E., 2013. Improvements in ^{230}Th dating, ^{230}Th and ^{234}U half-life values, and U–Th isotopic measurements by multi-collector inductively coupled plasma mass spectrometry. Earth and Planetary Science Letters, **371**: 82–91.

Crossey, L.J., Fischer, T.P., Patchett, P.J., Karlstrom, K.E., Hilton, D.R., Newell, D.L., Huntoon, P., Reynolds, A.C., de Leeuw, G.A.M., 2006. Dissected hydrologic system at the Grand Canyon: interaction between deeply derived fluids and plateau aquifer waters in modern springs and travertine. Geology, **34**: 25–28.

Çağatay, M.N., Öğretmen, N., Damcı, E., Stockhecke, M., Sancar, Ü., Eriş, K.K., Özeren, S., 2014. Lake level and climate records of the last 90 ka from the Northern Basin of Lake Van, eastern Turkey. Quaternary Science Reviews, **104**: 97–116.

Çukur, D., Krastel, S., Schmincke, H.-U., Sumita, M., Çağatay, M.N., Meydan, A.F., Damcı, E., Stockhecke, M., 2014a. Seismic stratigraphy of the lake Van, eastern Turkey. Quaternary Science Reviews, **104**: 63–84.

D'Alessandro, W., Giammanco, S., Bellomo, S., Parello, F., 2007. Geochemistry and mineralogy of travertine deposits of the SW flank of Mt. Etna (Italy): relationships with past volcanic and degassing activity. Journal of Volcanology and Geothermal Research, **165:** 64–70.

Djamali, M., De Beaulieu, J.-L., Shah-Hosseini, M., Andrieu-Ponel, V., Ponel, P., Amini, A., Akhani, H., Leroy, S. A., Stevens, L., Lahijani, H., Brewer, S., 2008. A late Pleistocene long pollen record from Lake Urmia, NW Iran. Quaternary Research, **69**: 413–420.

Djamali, M., Baumel, A., Brewer, S., Jackson, S.T., Kadereit, J.W., López-Vinyallonga, S., Simakova, A., 2012. Ecological implications of Cousinia Cass. (Asteraceae) persistence through the last two glacial–interglacial cycles in the continental Middle East for the Irano-Turanian flora. Review of Palaeobotany and Palynology, **172**: 10–20.

Dominguez-Villar, D., Vazquez-Navarro, J.A., Cheng, H., Edwards, R.L., 2011. Freshwater tufa record from Spain supports evidence for the past interglacial being wetter than the Holocene in the Mediterranean region. Global and Planetary Change, **77**: 129–141.

Erdoğan, O., Özvan, A., 2015. Evaluation of strength parameters and quality assessment of different lithotype levels of Edremit (Van) Travertine (Eastern Turkey). Journal of African Earth Science, **106**: 108–117.

Faccenna, C., Soligo, M., Billi, A., De Filippis, L., Funiciello, R., Rossetti, C., Tuccimei, P., 2008. Late Pleistocene depositional cycles of the Lapis Tiburtinus travertine (Tivoli, Central Italy): possible influence of climate and fault activity. Global and Planetary Change, **63**: 299–308.

Folk, R.L., Chafetz, H.S., Tiezzi, P.A., 1985. Bizarre forms of depositional and diagenetic calcite in hot-spring travertines, central Italy. SEPM Special Publication, **36**: 349–369.

Ford, T.D., Pedley, H.M., 1996. A review of tufa and travertine deposits of the world. Earth-Science Reviews, **41**: 117–175.

Fouke, B.W., Farmer, J.D., Des Marais, D.J., Pratt, L., Sturchio, N.C., Burns, P.C., Discipulo, M.K., 2000. Depositional facies and aqueous-solid geochemistry of travertine-depositing hot springs (Angel Terrace, Mammoth Hot Springs, Yellowstone National Park, U.S.A.). Journal of Sedimentary Research, **70**: 565–585.

Gandin, A. Capezzuoli, E., 2008. Travertine *versus* calcareous tufa: distinctive petrologic features and stable isotope signatures. Italian Journal of Quaternary Science, **21**: 125–136.

Gradziński, M., 2010. Factors controlling growth of modern tufa: results of a feld experiment. Geological Society Special Publications, **336**: 143–191.

Gradziński, M., Wróblewski, W., Duliński, M., Hercman, H., 2014. Earthquake-affected development of a travertine ridge. Sedimentology, **61:** 238–263.

Gradziński, M., Bella, P., Holúbek, P., 2018. Constructional caves in freshwater limestone: a review of their origin, classification, significance and global occurrence. Earth-Science Reviews, **185:** 179–201.

Griffiths, H.I., Pedley, H.M., 1995. Did changes in the late last glacial and early Holocene atmosphere CO_2 concentrations control the rates of tufa precipitation? Holocene, **52**: 238–242.

Glover, C., Robertson, A.H.F., 2003. Origin of tufa (cool-water carbonate) and related terraces in the Antalya area, SW Turkey. Geological Journal, **38**: 329–358.

Goudie, A.S.,Viles, H.A., Pentecost, A., 1993. The late-Holocene tufa decline in Europe. Holocene, **3**: 181–186.

Groff, F., Shevenell, L., 1987. Travertine deposits of Soda Dam, New Mexico, and their implications for the age and evolution of the Valles Caldera hydrothermal system. GSA Bulletin, **99**: 292–305.

Guido, D.M., Channing, A., Campbell, K.A., Zamuner, A., 2010. Jurassic geothermal landscapes and fossil ecosystems at San Agustín, Patagonia, Argentina. Journal of the Geological Society, **167**: 11–20.

Guido, D.M., Campbell, K.A., 2011. Jurassic hot spring deposits of the Deseado Massif (Patagonia, Argentina): characteristics and controls on regional distribution. Journal of Volcanology and Geothermal Research, **203**: 35–47.

Guo, L., Riding, R., 1998. Hot-spring travertine facies and sequences, Late Pleistocene Rapolano Terme, Italy. Sedimentology, **45**: 163–180.

Giustini, F., Brilli, M., Mancini, M., 2018. Geochemical study of travertines along middle-lower Tiber valley (central Italy): gene-

sis, palaeo-environmental and tectonic implications. International Journal of Earth Science, **107**: 1321–1342.

Gülyüz, E., Durak, H., Özkaptan, M., Krijgsman, W., 2019. Paleomagnetic constraints on the early Miocene closure of the southern Neo-Tethys (Van region; East Anatolia): inferences for the timing of Eurasia-Arabia collision. Global and Planetary Change, **185**, 103089.

Heimann, A., Sass, E., 1989. Travertines in the northern Hula Valley, Israel. Sedimentology, **36**: 95–108.

Helvacı, C., Griffin, W.L., 1985. Rb-Sr geochronology of the Bitlis Massif, Avnik (Bingöl) area, SE Turkey. Geological Society Special Publications, **17**: 403–413.

Henchiri, M., Ahmed, W.B., Brogi, A., Alcicek, M.C., Benassi, R., 2017. Evolution of Pleistocene travertine depositional system from terraced slope to fissure-ridge in a mixed travertine-alluvial succession (Jebel El Mida, Gafsa, southern Tunisia). Geodinamica Acta, **29**: 20–41.

Huybers, P., Langmuir, C., 2009. Feedback between deglaciation, volcanism, and atmospheric CO_2. Earth and Planetary Science Letters, **286**: 479–491.

Irion, G., Müller, G., 1968. Mineralogy, petrology and chemical composition of some calcareous tufa from the Swäbische Alb, Germany. In: Recent Developments in Carbonate Sedimentology in Central Europe (eds. G. Müller and G.M. Friedman): 157–171. Springer, Berlin.

Jones, B., Renaut, R.W., 2010. Calcareous spring deposits in continental settings. Developments in Sedimentology, **61:** 177–224.

Julia, R. 1983. Travertines. AAPG Memoir, **33**: 64–72.

Kadıoğlu, M., Şen, Z., Batur, E., 1997. The greatest soda-water lake in the world and how it is influenced by climatic change. Annales Geophysicae, **15**: 1489–1497.

Kartal, R.F., Kadiroğlu, F.T., Turkoğlu, M., Kaplan, M., Yanık, K., Zunbul, S., Kılıc, T., Demir, M., İde, A., Karaağac, D., 2012. Evaluation of aftershock activity of Van Earthquake, September, 23, 2011. In: 65th Geological Congress of Turkey, 2–6 April 2012, Ankara–Turkey. Abstracts Book, p. 21.

Keskin, M., 2003. Magma generation by slab steepening and breakoff beneath a subduction accretion complex: an alternative model for collision-related volcanism in Eastern Anatolia,Turkey. Geophysical Research Letters, **30**: 8046–8050.

Kind, R., Eken, T., Tilmann, F., Sodoudi, F., Taymaz, T., Bulut, F., Yuan, X., Can, B., Schneider, F., 2015. Thickness of the lithosphere beneath Turkey and surroundings from Sreceiver functions. Solid Earth, **6**: 971–984.

Kitano, Y., 1963. Geochemistry of calcareous deposits found in hot springs. Journal of Earth Science, Nagoya University, **11**: 68–100.

Koban, C.G., Schweigert, G., 1993. Microbial origin of travertine fabrics – two examples from southern Germany (Pleistocene Stuttgart travertines and Miocene Riedoschingen travertine). Facies, **29**: 251–264.

Koçyiğit, A., 2013. New field and seismic data about the intraplate strike-slip deformation in Van region, east Anatolian plateau, E Turkey. Journal of Asian Earth Science, **62**: 586–605.

Kraus, M., 1999. Paleosols in clastic sedimentary rocks: their geologic applications. Earth-Science Reviews, **47**: 41–70.

Kronfeld, J., Voggel, J.C., Rosenthal, E., Weinstein-Evron, M., 1988. Age and paleoclimatic implications of the Bet Shean travertines. Quaternary Research, **30**: 298–303.

Kuzucuoğlu, C., Christol, A., Mouralis, D., Doğu, A.-F., Akköprü, E., Fort, M., Brunstein, D., Zorer, H., Fontugne, M., Karabiyikoglu, M., Scaillet, S., Reyss, J.-L., Guillou, H., 2010. Formation of the Upper Pleistocene terraces of Lake Van (Turkey). Journal of Quaternary Sciences, **25**: 1124–1137.

Landmann, G., Reimer, A., Lemcke, G., Kempe, S., 1996a. Dating Late Glacial abrupt climate changes in the 14,570 yr long continuous varve record of Lake Van, Turkey. Palaeogeography, Palaeoclimatology, Palaeoecology, **122**: 107–118.

Landmann, G., Reimer, A., Kempe, S., 1996b. Climatically induced lake level changes at Lake Van, Turkey, during the Pleistocene/Holocene transition. Global Biogeochemical Cycles, **10**: 797–808.

Lebedev, V.A., Sharkov, E.V., Keskin, M., Oyan, V., 2010. Geochronology of the Late Cenozoic volcanism in the area of Van Lake (Turkey): an example of the developmental dynamics for magmatic processes. Doklady Earth Sciences, **433**: 1031–1037.

Lisiecki, L.E., Raymo, M.E., 2005. A Pliocene-Pleistocene stack of 57 globally distributed benthic ^{18}O records. Paleoceanography, **20**, PA1003, Data archived at the World Data Center for Paleoclimatology, Boulder, Colorado, USA.

Litt, T., Krastel, S., Sturm, M., Kipfer, R., Örcen, S., Heumann, G., Franz, S.O., Ülgen, U.B., Niessen, F., 2009. 'PALEOVAN', International Continental Scientific Drilling Program (ICDP): site survey results and perspectives. Quaternary Science Reviews, **28**: 1555–1567.

Litt, T., Anselmetti, F.S., Çağatay, M.N., Kipfer, R., Krastel, S., Schmincke, H.U., Sturm, M., 2011. A 500,000-year-long sediment archive drilled in eastern Anatolia. American Geophysics Union Eos Transition, **92**: 477–479.

Litt, T., Pickarski, N., Heumann, G., 2014. A 600,000 year long continental pollen record from Lake Van, Eastern Anatolia (Turkey). Quaternary Science Revievs, **104**: 30–41.

Luo, L., Wen, H., Capezzuoli, E., 2021. Travertine deposition and diagenesis in Ca-deficiency perched hot spring systems: A case from Shihuadong, Tengchong, China. Sedimentary Geology, **414**: 105827.

Martin-Bello, L., Arenas, C., Jones, B., 2019. Lacustrine stromatolites: Useful structures for environmental interpretation – an example from the Miocene Ebro Basin. Sedimentology, **66**: 2098–2133.

Martinez-Diaz, J., Hernández-Enrile, J., 2001. Using travertine deformations to characterize paleoseismic activity along an active oblique-slip fault: The Alhama de Murcia fault (Betic Cordillera, Spain). Acta Geológica Hispánica, **36**: 3–4.

Mesci, B.L., Gürsoy, H, Tatar, O., 2008. The evolution of travertine masses in the Sivas area (central Turkey) and their relationships to active tectonics. Turkish Journal of Earth Sciences, **17**: 219–240.

Mesci, B.L., Tatar, O., Piper, J.D.A., Gürsoy, H., Altunel, E., Crowley, S., 2013. The efficacy of travertine as a palaeoenvironmental indicator: palaeomagnetic study of neotectonic examples from Denizli, Turkey. Turkish Journal of Earth Sciences, **22**: 191–203.

Mohajjel, M., Taghipour, K., 2014. Quaternary travertine ridges in the Lake Urmia area: Active extension in NW Iran. Turkish Journal of Earth Sciences, **23**: 602–614.

Morrison, R.B., 1967. Principles of Quaternary soil stratigraphy. Proceeding of International Associations, Quaternary Research (INQUA), **8**: 1–113.

Muir-Wood, R., 1993. Neohydrotectonics. Zeitschrift für Geomorphologie Supplement-Band, **94**: 275–284.

Nyssen, J., Poesen, J., Moeyersons, J., Deckers, J., Haile, M., Lang, A., 2004. Human impact on the environment in the Ethiopian and Eritrean highlands – a state of the art. Earth Science Reviews, **64**: 273–320.

Owen, R.B., Renaut, R.W., Stamatakis, M.G., 2010. Diatomaceous sedimentation in late Neogene lacustrine basins of western Macedonia. Greece. Journal of Paleolimnology, **44**: 343–359.

Oyan, V., 2018a. Ar\Ar dating and petrogenesis of the Early Miocene Taţkapý-Mecitli (Erciţ-Van) granitoid, Eastern Anatolia Collisional Zone, Turkey. Journal of Asian Earth Sciences, **158**: 210–226.

Oyan, V., 2018b. Geochemical and petrologic evolution of Otlakbaţý basaltic volcanism to the east of Lake Van. Bulletin of the Mineral Research and Exploration. **157**: 1–21.

Oyan, V., Keskin, M., Lebedev, V.A., Chugaev, A.V., Sharkov, E.V., 2016. Magmatic evolution of the Early Pliocene Etrüsk stratovolcano, Eastern Anatolian Collision Zone, Turkey. Lithos, **256–257**: 88–108.

Oyan, V., Keskin, M., Lebedev, V.A., Chugaev, A.V., Sharkov, E.V., Ünal, E., 2017. Petrology and geochemistry of the Quater-

nary mafic volcanism in the north-east of Lake Van, Eastern Anatolian Collision Zone, Turkey. Journal of Petrology, **58**: 1701–1728.

Ön, Z. B., Özeren, M. S., 2019. Temperature and precipitation variability in eastern Anatolia: results from independent component analysis of Lake Van sediment data spanning the last 250 kyr BP. Quaternary International, **514**: 119–129.

Özdemir, Y., Güleç, N., 2014. Geological and geochemical evoluation of Suphan stratovolcano Eastern Anatolia, Turkey: evidence for the lithosphere-asthenosphere interaction on post collisional volcanism. Journal of Petrology, **55**: 37–62.

Özacar, A.A., Gilbert, H., Zandt, G., 2008. Upper mantle discontinuity structure beneath East Anatolian Plateau (Turkey) from receiver functions. Earth and Planetary Science Letters, **269**: 426–434.

Özdemir, Y., Karaoğlu, Ö., Tolluođlu, A.Ü., Güleç, N., 2006. Volcanostratigraphy and petrogenesis of the Nemrut stratovolcano (East Anatolian High Plateau): the most recent postcollisional volcanism in Turkey. Chemical Geology, **226**: 189–211.

Özkaymak, C., Sozbilir, H., Bozkurt, E., Dirik, K., Topal, T., Alan, H., Cağlan, D., 2012. Seismic geomorphology of October 23, 2011 Tabanlı-Van Earthquake and its relation to active tectonics of East Anatolia (in Turkish with English summary). Journal of Geological Engineering, **35**: 175–199.

Özkul, M., Alçiçek, M.C., Heybeli, H., Semiz, B., Erten, H., 2001. Depositional features of Denizli hot spring travertines and their appraisement in view marbling (in Turkish with English summary). III. Turkey Marble Symposium (Mersem'2001) Proceeding Book, 57–72, Afyon, Turkey.

Özkul, M., Varol, B., Alçiçek, M.C., 2002. Depositional environments and petrography of the Denizli travertines. Bulletin of Mineral Research Exploring, **125**: 13–29.

Özkul, M., Gökgöz, A., Horvatinčić, N., 2010. Depositional properties and geochemistry of Holocene perched springline tufa deposits and associated spring waters: a case study from the Denizli province, Western Turkey. Geological Society Special Publications, **336**: 245–262.

Özkul, M., Gökgöz, A., Sandor, K., Baykara, M.O., Shen, C.C., Chang, Y.W., Kaya, A., Hançer, M., Aratman, C., Taylan, A., Örü, Z., 2014. Sedimentological and geochemical characteristics of a fluvial travertine: a case from the eastern Mediterranean region. Sedimentology, **61**: 291–318.

Özkul, M., Kele, S., Gökgöz, A., Shen, C.C., Jones, B., Baykara, M.O., Fürizs, I., Nemeth, T., Chang, Y.-W., Alçiçek, M.C., 2013. Comparison of the Quaternary travertine sites in the Denizli Extensional Basin based on their depositional and geochemical data. Sedimentary Geology, **294**: 179–204.

Pazonyi, P., Kordos, L., Magyari, E., Marinova, E., Füköh, L., Venczel, M., 2014. Pleistocene vertebrate faunas of the Sütto travertine complex (Hungary). Quaternary International, **319**: 50–63.

Pedley, H.M., 1990. Classification and environmental models of cool freshwater tufas. Sedimentary Geology, **68**: 143–154.

Pedley, M., 2009. Tufas and travertines of the Mediterranean region: a testing ground for freshwater carbonate concepts and developments. Sedimentology, **56**: 221–246.

Pedley, H.M., Rogerson, M., Middleton, R., 2009. The growth and morphology of freshwater calcite precipitates from in vitro mesocosm flume experiments. Sedimentology, **56**: 511–527.

Pentecost, A., 1981. The tufa deposits of the Malham District. Field Study, **5**: 365–387.

Pentecost, A., Viles, H.A., 1994. A review and reassessment of travertine classification. Géographie Physique et Quaternaire, **48**: 305–314.

Pentecost, A., 1995. The Quaternary travertine deposits of Europe and Asia Minor. Quaternary Science Reviews, **14**: 1005–1028.

Pentecost, A., 2005. Travertine. Springer, Berlin.

Pentecost, A., Merritt, R., Carter, C., 2014. Growth and calcification of Vaucheria (Xanthophyta) on a travertine surface in a temperate freshwater setting. European Journal of Phycology, **49**: 516–525.

Pecsi, M., 1995. Loess stratigraphy and Quaternary climatic change. Loess in Form, **3**: 23–30.

Pickarski, N., Kwiecien, O., Langgut, D., Litt, T., 2015. Abrupt climate and vegetation variability of eastern Anatolia during the last Glacial. Climate of the Past, **11**: 1491–1505.

Piper, J.D., Mesci, L.B., Gürsoy, H., Tatar, O., Davies, C.J., 2007. Palaeomagnetic and rock magnetic properties of travertine: its potential as a recorder of geomagnetic palaeosecular variation, environmental change and earthquake activity in the Sıcak Cermik geothermal field, Turkey. Physics of the Earth and Planetary Interiors, **161**: 50–73.

Retallack, G.J., 2014. Paleosols and paleoenvironments of early Mars. Geology, **42**: 755–758.

Richmond, G.M., 1962. Quaternary stratigraphy of the La Sal Mountains, Utah. U.S. Geological Survey Professional Paper, **324**.

Rogerson, M., Pedley, H.M., Wadhawan, J.D., Middleton, R., 2008. New insights into biological influence on the geochemistry of freshwater carbonate deposits. Geochimica et Cosmochimica Acta, **72**: 4976–4987.

Sağlam Selçuk, A., 2016. Evaluation of the relative tectonic activity in the eastern Lake Van basin, East Turkey. Geomorphology, **270**: 9–21.

Sheldon, N.D., Tabor, N.J., 2009. Quantitative paleoenvironmental and paleoclimatic reconstruction using paleosols. Earth-Science Reviews, **95**: 1–52.

Shen, C.-C., Wu, C.-C., Cheng, H., Edwards, R.L., Hsieh, Y.-T., Gallet, S., Chang, C.-C., Li, T.-Y., Lam, D.D., Kano, A., Hori, M., Spötl, C., 2012. High-precision and high-resolution carbonate ^{230}Th dating by MC-ICP-MS with SEM protocols. Geochimica et Cosmochimica Acta, **99**: 71–86.

Shen, C.-C., Cheng, H., Edwards, R.L., Moran, S.B., Edmonds, H.N., Hoff, J.A., Thomas, R.B., 2003. Measurement of attogram quantities of ^{231}Pa in dissolved and particulate fractions of seawater by isotope dilution thermal ionization mass spectroscopy. Analytical Chemistry, **75**: 1075–1079.

Sibson, R.H., Moore, J.M.M., Rankin, A.H., 1975. Seismic pumping a hydrothermal fluid transport mechanism. Journal of the Geological Society, **131:** 653–659.

Singer, A., Wieder, M., Gvirtzman, G., 1994. Paleoclimate deduced from some early Jurassic basalt-derived paleosols from northern Israel. Palaeogeography, Palaeoclimatology, Palaeoecology, **111:** 73–82.

Southard, A.R.,Miller, R.W.,1966.Parent material-clay relations in some northern Utah soils. Soil Science Society of America Journal, **30**: 97–101.

Steffensen, J.P., Andersen, K.K., Bigler, M., Clausen, H.B., Dahl-Jensen, D., Fischer, H., Goto-Azuma, K., Hansson, M., Johnsen, S.J., Jouzel, J., Masson-Delmotte, V., Popp, T., Rasmussen, S.O., Röthlisberger, R., Ruth, U., Stauffer, B., Siggaard-Andersen, M.L., Sveinbjörnsdóttir, A.E., Svensson, A.,White, J.W.C., 2008. High–resolution Greenland ice core data show abrupt climate change happens in few years. Science, **321**: 680–684.

Stevens, L.R., Djamali, M., Andrieu-Ponel, V., de Beaulieu, J.-L., 2012. Hydroclimatic variations over the last two glacial/interglacial cycles at Lake Urmia, Iran. Journal of Paleolimnology, **47**: 645–660.

Stockhecke, M., Sturm, M., Brunner, I., Schmincke, H.U., Sumita, M., Kipfer, R., Çukur, D., Kwiecien, O., Anselmetti, F.S., 2014. Sedimentary evolution and environmental history of Lake Van (Turkey) over the past 600,000 years. Sedimentology, **61**: 1830–1861.

Svensson, A., Andersen, K.K., Bigler, M., Clausen, H.B., Dahl-Jensen, D., Davies, S.M., Johnsen, S.J., Muscheler, R., Parrenin, F., Rasmussen, S.O., Röthlisberger, R., Seierstad, I., Steffensen, J.P., Vinther, B.M., 2008. A 60 000 year Greenland stratigraphic ice core chronology. Climate of the Past, **4**: 47–57.

Şaroğlu, F., Yılmaz, Y., 1986. Doğu Anadolu'da neotektonik donemdeki jeolojik evrim ve havza modelleri (in Turkish). Mineral Research Exploring Instute (MTA) Bulletin, **107**: 73–94.

Tabor, N.J., Myers, T.S., 2015. Paleosols as indicators of paleoenvironment and paleoclimate. Annual Reviews Earth Science, **43**: 333–361.

Tagliasacchi-Toker, E., 2018. Orta-geç Pleistosen Gürlek-Kocabaş (Denizli) ve Örtülü (Afyon) travertenlerinin paleoçevresel gelişimi, SW. Türkiye (in Turkish). Türkiye Jeoloji Bülteni, **60**: 1–22.

Tlili, F., Ayari, A., Regaya, K.. 2021. Bio-mineral needle fiber calcite (NFC) in Tunisian Pleistocene calcretes (topology and crystallization). Journal of Earth System Science, **130**: 1–16.

Thomas, S.G., Tabor, N.J., Yang, W., Myers, T.S., Yang, Y., Wang, D., 2011. Palaeosol stratigraphy across the Permian–Triassic boundary, Bogda Mountains, NW China: implications for palaeoenvironmental transition through Earth's largest mass extinction. Palaeogeography, Palaeoclimatology, Palaeoecology. **308**: 41–64.

Toker, M., 2013. Time-dependent analysis of aftershock events and structural impacts on intraplate crustal seismicity of the Van earthquake (Mw 7.1, 23 October 2011), E-Anatolia. Central European Journal of Geosciences, **5**: 423–434.

Toker, M., 2014. Discrete characteristics of the aftershock sequence of the 2011 Van earthquake. Journal of Asian Earth Science, **92**: 168-186.

Toker, M., Pınar, A., Tur, H., 2017. Source mechanisms and faulting analysis of the aftershocks in the Lake Erçek area (Eastern Anatolia, Turkey) during the 2011 Van event (Mw 7.1): implications for the regional stress field and ongoing deformation processes. Journal of Asian Earth Science, **150**: 73–86.

Ulusoy, İ., Çubukçu, H.E., Aydar, E., Labazuy, P., Ersoy, O., Şen, E., Alain, G., 2012. Volcanological evolution and caldera forming eruptions of Mt. Nemrut (Eastern Turkey). Journal of Volcanology and Geothermal Research, **245–246**: 21–39.

Utkucu, M., 2013. 23 October 2011 Van, Eastern Anatolia, earthquake (Mw 7·1) and seismotectonics of Lake Van area. Journal of Seismology, **17**: 783–805.

Utkucu, M., Kızılbuğa, S., Arman, H., 2017. Constraining fault rupture of the 27 November 2005 Qeshm Island (Iran) earthquake (M_W=6.0) in the Arabian Gulf from the inversion of the teleseismic broadband waveforms. Extended abstract, fourth international conference on engineering geophysics, proceedings book, October 9–12, 2017 United Arab Emirates University, Al Ain.

Van Noten, K., Topal, S., Baykara, O., Özkul, M., Claes, H., Aratman, C., Swennen, R., 2018. Pleistocene-Holocene tectonic reconstruction of the Ballýk travertine (Denizli Graben, SW Turkey): (de)formation of large travertine geobodies at intersecting grabens. Journal of Structural Geology **118**: 114–134.

Veysey, J., Fouke, B.W., Kandianis, M.T., Schickel, T.J., Johnson, R.W., Goldenfeld, N., 2008. Reconstruction of water temperature, pH, and flux of ancient hot springs from travertine depositional facies. Journal of Sedimentary Research, **78**: 69–76.

Viles, H.A., Goudie, A.S., 1990. Tufas, travertines and allied carbonate deposits. Progress in Physical Geography, **14**: 19–41.

Wick, L., Lemcke, G., Sturm, M., 2003. Evidence for Lateglacial and Holocene climatic change and human impact in eastern Anatolia: high-resolution pollen, charcoal, isotopic and geochemical records from the laminated sediments of Lake Van, Turkey. Holocene, **13**: 665–675.

Wolff, E.W., Chappellaz, J., Blunier, T., Rasmussen, S.O., Svensson, A., 2010. Millennial–scale variability during the last Glacial: the ice core record. Quaternary Science Reviews, **29**: 2828–2838.

Yeşilova, Ç., Güngör Yeşilova, P., Açlan, M., 2015a. Edremit (Van) Travertenlerinin Fasiyes Analizi (in Turkish). 68. Türkiye Jeoloji Kurultayı, 578–579, Ankara, Türkiye.

Yeşilova, Ç., Üner, S., Güngör Yeşilova, P., Açlan, M., Alırız, M.G., 2015b. Kuvaterner Yaşlı Edremit Travertenleri'nin Fasiyes Özellikleri ve Oluşum Ortamları (Van Gölü Havzası-Doğu Anadolu) (in Turkish). Traverten – Tufa Çalıştayı, Pamukkale Üniversitesi Mühendislik Fakültesi, Denizli: 54–55.

Yeşilova, Ç., 2019. Preliminary approach to paleogeographic properties of Edremit (Van) Travertines, eastern Turkey. IESCA, 7–11 October 2019, İzmir.

Yeşilova, Ç., Gülyüz, E., Ci-Rong, H., Chuan-Chou, S., 2019. Giant tufas of Lake Van record lake-level fluctuations and climatic changes in eastern Anatolia, Turkey. Palaeogeography, Palaeoclimatology, Palaeoecology, **533**: 1–9.

Zor, E., Gürbüz, C., Türkelli, N., Sandvol, E., Seber, D., Barazangi, M., 2003. The crustal structure of the East Anatolian Plateau from receiver functions. Geophysical Research Letters, **30**: 8044–8047.